

Microbiota Modulate Behavioral and Physiological Abnormalities Associated with Neurodevelopmental Disorders

Elaine Y. Hsiao,^{1,2,*} Sara W. McBride,¹ Sophia Hsien,¹ Gil Sharon,¹ Embriette R. Hyde,³ Tyler McCue,³ Julian A. Codelli,² Janet Chow,¹ Sarah E. Reisman,² Joseph F. Petrosino,³ Paul H. Patterson,^{1,4,*} and Sarkis K. Mazmanian^{1,4,*}

¹Division of Biology and Biological Engineering, California Institute of Technology, Pasadena, CA 91125, USA

²Division of Chemistry and Chemical Engineering, California Institute of Technology, Pasadena, CA 91125, USA

³Alkek Center for Metagenomics and Microbiome Research, Baylor College of Medicine, Houston, TX 77030, USA

⁴These authors contributed equally to this work

*Correspondence: ehsiao@caltech.edu (E.Y.H.), php@caltech.edu (P.H.P.), sarkis@caltech.edu (S.K.M.)

<http://dx.doi.org/10.1016/j.cell.2013.11.024>

SUMMARY

Neurodevelopmental disorders, including autism spectrum disorder (ASD), are defined by core behavioral impairments; however, subsets of individuals display a spectrum of gastrointestinal (GI) abnormalities. We demonstrate GI barrier defects and microbiota alterations in the maternal immune activation (MIA) mouse model that is known to display features of ASD. Oral treatment of MIA offspring with the human commensal *Bacteroides fragilis* corrects gut permeability, alters microbial composition, and ameliorates defects in communicative, stereotypic, anxiety-like and sensorimotor behaviors. MIA offspring display an altered serum metabolomic profile, and *B. fragilis* modulates levels of several metabolites. Treating naive mice with a metabolite that is increased by MIA and restored by *B. fragilis* causes certain behavioral abnormalities, suggesting that gut bacterial effects on the host metabolome impact behavior. Taken together, these findings support a gut-microbiome-brain connection in a mouse model of ASD and identify a potential probiotic therapy for GI and particular behavioral symptoms in human neurodevelopmental disorders.

INTRODUCTION

Neurodevelopmental disorders are characterized by impaired brain development and behavioral, cognitive, and/or physical abnormalities. Several share behavioral abnormalities in sociability, communication, and/or compulsive activity. Most recognized in this regard is autism spectrum disorder (ASD), a serious neurodevelopmental condition that is diagnosed based on the presence and severity of stereotypic behavior and deficits in language and social interaction. The reported incidence of ASD has rapidly increased to 1 in 88 births in the United States as of 2008

(Autism and Developmental Disabilities Monitoring Network Surveillance Year 2008 Principal Investigators and CDC, 2012), representing a significant medical and social problem. However, therapies for treating core symptoms of autism are limited. Much research on ASD has focused on genetic, behavioral, and neurological aspects of disease, though the contributions of environmental risk factors (Hallmayer et al., 2011), immune dysregulation (Onore et al., 2012), and additional peripheral disruptions (Kohane et al., 2012) in the pathogenesis of ASD have gained significant attention.

Among several comorbidities in ASD, gastrointestinal (GI) distress is of particular interest, given its reported prevalence (Buie et al., 2010; Coury et al., 2012) and correlation with symptom severity (Adams et al., 2011). While the standardized diagnosis of GI symptoms in ASD is yet to be clearly defined, clinical as well as epidemiological studies have reported abnormalities such as altered GI motility and increased intestinal permeability (Boukthir et al., 2010; D'Eufemia et al., 1996; de Magistris et al., 2010). Moreover, a recent multicenter study of over 14,000 ASD individuals reveals a higher prevalence of inflammatory bowel disease (IBD) and other GI disorders in ASD patients compared to controls (Kohane et al., 2012). GI abnormalities are also reported in other neurological diseases, including Rett syndrome (Motil et al., 2012), cerebral palsy (Campanozzi et al., 2007), and major depression (Graff et al., 2009). The causes of these GI problems remain unclear, but one possibility is that they may be linked to gut bacteria.

Indeed, dysbiosis of the microbiota is implicated in the pathogenesis of several human disorders, including IBD, obesity, and cardiovascular disease (Blumberg and Powrie, 2012), and several studies report altered composition of the intestinal microbiota in ASD (Adams et al., 2011; Finegold et al., 2010; Finegold et al., 2012; Kang et al., 2013; Parracho et al., 2005; Williams et al., 2011; Williams et al., 2012). Commensal bacteria affect a variety of complex behaviors, including social, emotional, and anxiety-like behaviors, and contribute to brain development and function in mice (Collins et al., 2012; Cryan and Dinan, 2012) and humans (Tillisch et al., 2013). Long-range interactions between the gut microbiota and brain underlie the ability of microbe-based therapies to treat symptoms of multiple sclerosis

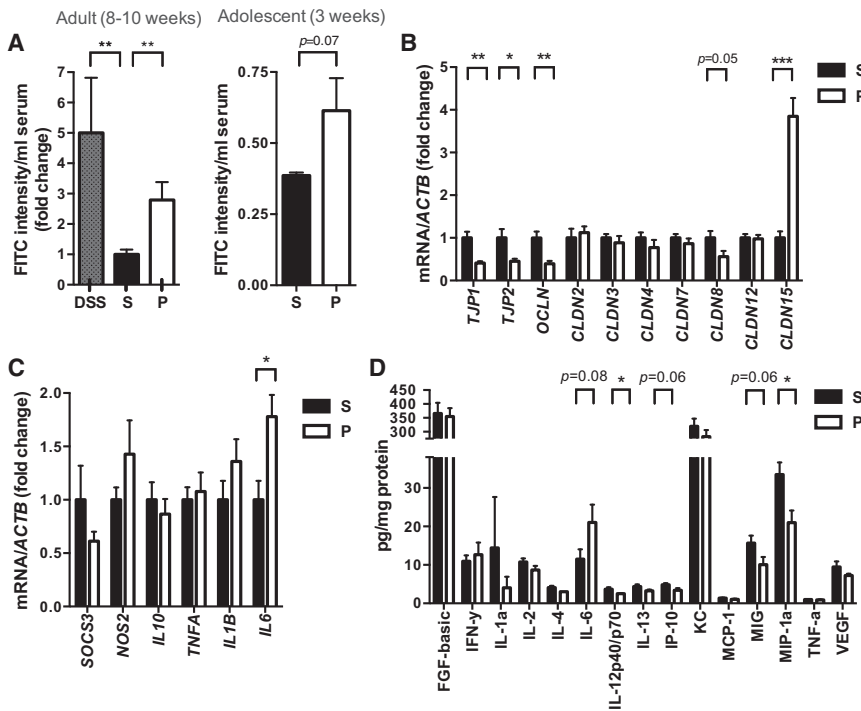


Figure 1. MIA Offspring Exhibit GI Barrier Defects and Abnormal Expression of Tight Junction Components and Cytokines

(A) Intestinal permeability assay, measuring FITC intensity in serum after oral gavage of FITC-dextran. Dextran sodium sulfate (DSS): n = 6, S (saline+vehicle): adult n = 16; adolescent n = 4, P (poly(I:C)+vehicle): adult n = 17; adolescent n = 4. Data are normalized to saline controls. (B) Colon expression of tight junction components relative to β -actin. Data for each gene are normalized to saline controls. n = 8/group. (C) Colon expression of cytokines and inflammatory markers relative to β -actin. Data for each gene are normalized to saline controls. n = 6–21/group. (D) Colon protein levels of cytokines and chemokines relative to total protein content. n = 10/group. For each experiment, data were collected simultaneously for poly(I:C)+*B. fragilis* treatment group (See Figure 3). See also Figure S1.

and depression in mice (Bravo et al., 2011; Ochoa-Repáraz et al., 2010), and the reported efficacy of probiotics in treating emotional symptoms of chronic fatigue syndrome and psychological distress in humans (Messaudi et al., 2011; Rao et al., 2009).

Based on the emerging appreciation of a gut-microbiome-brain connection, we asked whether modeling some of the behavioral features of ASD in a mouse model also causes GI abnormalities. Several mouse models of genetic and/or environmental risk factors are used to study ASD. We utilize the maternal immune activation (MIA) model, which is based on large epidemiological studies linking maternal infection to increased autism risk in the offspring (Atladóttir et al., 2010; Gorrindo et al., 2012). A number of studies link increased ASD risk to familial autoimmune disease (Atladóttir et al., 2009; Comi et al., 1999) and elevated levels of inflammatory factors in the maternal blood, placenta, and amniotic fluid (Abdallah et al., 2013; Brown et al., 2013; Croen et al., 2008). Modeling MIA in mice by injecting pregnant dams with the viral mimic poly(I:C) yields offspring that exhibit the core communicative, social, and stereotyped impairments relevant to ASD, as well as a common autism neuropathology—a localized deficiency in cerebellar Purkinje cells (Malkova et al., 2012; Shi et al., 2009). Furthermore, pregnant monkeys exposed to poly(I:C) yield offspring with symptoms of ASD (Bauman et al., 2013). Although several environmental and genetic risk factors for ASD have been investigated in pre-clinical models, GI abnormalities have not been reported. We show herein that offspring of MIA mice, which display behavioral abnormalities, have defects in intestinal integrity and alterations in the composition of the commensal microbiota that are analogous to features reported in human ASD. To explore the potential contribution of GI complications to these symptoms, we

examine whether treatment with the gut bacterium *Bacteroides fragilis*, demonstrated to correct GI pathology in mouse models of colitis (Mazmanian et al., 2008) and to protect against neuroinflammation in mouse models of multiple sclerosis (Ochoa-Repáraz et al., 2010), impacts ASD-related GI and/or behavioral abnormalities in MIA offspring. Our study reflects a mechanistic investigation of how alterations in the commensal microbiota impact behavioral abnormalities in a mouse model of neurodevelopmental disease. Our findings suggest that targeting the microbiome may represent an approach for treating subsets of individuals with behavioral disorders, such as ASD, and comorbid GI dysfunction.

RESULTS

Offspring of Immune-Activated Mothers Exhibit GI Symptoms of Human ASD

Subsets of ASD children are reported to display GI abnormalities, including increased intestinal permeability or “leaky gut” (D’Eufemia et al., 1996; de Magistris et al., 2010; Ibrahim et al., 2009). We find that adult MIA offspring, which exhibit a number of behavioral and neuropathological symptoms of ASD (Malkova et al., 2012), also have a significant deficit in intestinal barrier integrity, as reflected by increased translocation of FITC-dextran across the intestinal epithelium, into the circulation (Figure 1A, left). This MIA-associated increase in intestinal permeability is similar to that of mice treated with dextran sodium sulfate (DSS), which induces experimental colitis (Figure 1A, left). Deficits in intestinal integrity are detectable in 3-week-old MIA offspring (Figure 1A, right), indicating that the abnormality is established during early life. Consistent with the leaky gut phenotype, colons from adult MIA offspring contain decreased gene expression of *TJP1*, *TJP2*, *OCLN*, and *CLDN8* and increased expression of *CLDN15* (Figure 1B). Deficient expression of *TJP1* is also observed in small intestines of adult MIA

offspring (Figure S1A available online), demonstrating a widespread defect in intestinal barrier integrity.

Gut permeability is commonly associated with an altered immune response (Turner, 2009). Accordingly, colons from adult MIA offspring display increased levels of interleukin-6 (IL-6) mRNA and protein (Figures 1C and 1D) and decreased levels of the cytokines/chemokines IL-12p40/p70 and MIP-1 α (Figure 1D). Small intestines from MIA offspring also exhibit altered cytokine/chemokine profiles (Figure S1C). Changes in intestinal cytokines are not accompanied by overt GI pathology, as assessed by histological examination of gross epithelial morphology from hematoxylin- and eosin-stained sections (data not shown). Overall, we find that adult offspring of immune-activated mothers exhibit increased gut permeability and abnormal intestinal cytokine profiles.

MIA Offspring Display Dysbiosis of the Gut Microbiota

Abnormalities related to the microbiota have been identified in ASD individuals, including disrupted community composition (Adams et al., 2011; Finegold et al., 2010; Finegold et al., 2012; Parracho et al., 2005; Williams et al., 2011; Williams et al., 2012), although it is important to note that a well-defined ASD-associated microbial signature is lacking thus far. To evaluate whether MIA induces microbiota alterations, we surveyed the fecal bacterial population by 16S rRNA gene sequencing of samples isolated from adult MIA or control offspring. Alpha diversity, i.e., species richness and evenness, did not differ significantly between control and MIA offspring, as measured by several indices (Figures S2A and S2B). In contrast, unweighted UniFrac analysis, which measures the degree of phylogenetic similarity between microbial communities, reveals a strong effect of MIA on the gut microbiota of adult offspring (Figure 2). MIA samples cluster distinctly from controls by principal coordinate analysis (PCoA) and differ significantly in composition (Table S3, with ANOSIM $R = 0.2829$, $p = 0.0030$), indicating robust differences in the membership of gut bacteria between MIA offspring and controls (Figure 2A). The effect of MIA on altering the gut microbiota is further evident when sequences from the classes Clostridia and Bacteroidia, which account for approximately 90.1% of total reads, are exclusively examined by PCoA ($R = 0.2331$, $p = 0.0070$; Figure 2B), but not when Clostridia and Bacteroidia sequences are specifically excluded from PCoA of all other bacterial classes ($R = 0.1051$, $p = 0.0700$; Figure 2C). This indicates that changes in the diversity of Clostridia and Bacteroidia operational taxonomic units (OTUs) are the primary drivers of gut microbiota differences between MIA offspring and controls.

Sixty-seven of the 1,474 OTUs detected across any of the samples discriminate between treatment groups, including those assigned to the bacterial families *Lachnospiraceae*, *Ruminococcaceae*, *Erysipelotrichaceae*, *Alcaligenaceae*, *Porphyromonadaceae*, *Prevotellaceae*, *Rikenellaceae*, and unclassified Bacteroidales (Figure 2D and Table S1). Of these 67 discriminatory OTUs (relative abundance: $13.3\% \pm 1.65\%$ control, $15.93\% \pm 0.62\%$ MIA), 19 are more abundant in the control samples and 48 are more abundant in MIA samples. Consistent with the PCoA results (Figures 2A–2C), the majority of OTUs that discriminate MIA offspring from controls are assigned to the

classes Bacteroidia (45/67 OTUs or 67.2%; $12.02\% \pm 1.62\%$ control, $13.48\% \pm 0.75\%$ MIA) and Clostridia (14/67 OTUs or 20.9%; $1.00\% \pm 0.25\%$ control, $1.58\% \pm 0.34\%$ MIA). Interestingly, *Porphyromonadaceae*, *Prevotellaceae*, unclassified Bacteroidales (36/45 discriminatory Bacteroidial OTUs or 80%; $4.46\% \pm 0.66\%$ control, $11.58\% \pm 0.86\%$ MIA), and *Lachnospiraceae* (8/14 discriminatory Clostridial OTUs or 57%; $0.28\% \pm 0.06\%$ control, $1.13\% \pm 0.26\%$ MIA) were more abundant in MIA offspring. Conversely, *Ruminococcaceae* (2 OTUs), *Erysipelotrichaceae* (2 OTUs), and the beta Proteobacteria family *Alcaligenaceae* (2 OTUs) were more abundant in control offspring (Figure 2D and Table S1; $0.95\% \pm 0.31\%$ control, $0.05\% \pm 0.01\%$ MIA). This suggests that specific *Lachnospiraceae*, along with other Bacteroidial species, may play a role in MIA pathogenesis, while other taxa may be protective. Importantly, there is no significant difference in the overall relative abundance of Clostridia ($13.63\% \pm 2.54\%$ versus $14.44\% \pm 2.84\%$; $p = 0.8340$) and Bacteroidia ($76.25\% \pm 3.22\%$ versus $76.22\% \pm 3.46\%$; $p = 0.9943$) between MIA offspring and controls (Figure 2E, left), indicating that alterations in the membership of Clostridial and Bacteroidial OTUs drive major changes in the gut microbiota between experimental groups.

Overall, we find that MIA leads to dysbiosis of the gut microbiota, driven primarily by alterations in specific OTUs of the bacterial classes Clostridia and Bacteroidia. Changes in OTUs classified as *Lachnospiraceae* and *Ruminococcaceae* of the order Clostridiales parallel select reports of increased *Clostridium* species in the feces of subjects with ASD (Finegold et al., 2012). Altogether, modeling MIA in mice induces not only behavioral and neuropathological features of ASD (Malkova et al., 2012; Shi et al., 2009) but also microbiome changes as described in subsets of ASD individuals.

Bacteroides fragilis Improves Gut Barrier Integrity in MIA Offspring

Gut microbes play an important role in the development, maintenance and repair of the intestinal epithelium (Turner, 2009). To determine whether targeting the gut microbiota could impact MIA-associated GI abnormalities, we treated mice with the human commensal *B. fragilis* at weaning, and tested for GI abnormalities at 8 weeks of age. *B. fragilis* has previously been shown to ameliorate experimental colitis (Mazmanian et al., 2008; Round and Mazmanian, 2010). Remarkably, *B. fragilis* treatment corrects intestinal permeability in MIA offspring (Figure 3A). In addition, *B. fragilis* treatment ameliorates MIA-associated changes in expression of CLDNs 8 and 15, but not *TJP1*, *TJP2*, or *OCLN* (Figure 3B). Similar changes are observed in protein levels of CLDNs 8 and 15 in the colon, with restoration by *B. fragilis* treatment (Figures 3C and 3D). No effects of *B. fragilis* on tight junction expression are observed in the small intestine (Figure S1B), consistent with the fact that *Bacteroides* species are predominantly found in the colon. Finally, the presence of GI defects prior to probiotic administration (Figure 1A, right) suggests that *B. fragilis* may treat, rather than prevent, this pathology in MIA offspring.

B. fragilis treatment also restores MIA-associated increases in colon IL-6 mRNA and protein levels (Figures 3E and 3F). Levels of other cytokines are altered in both colons and small intestines of

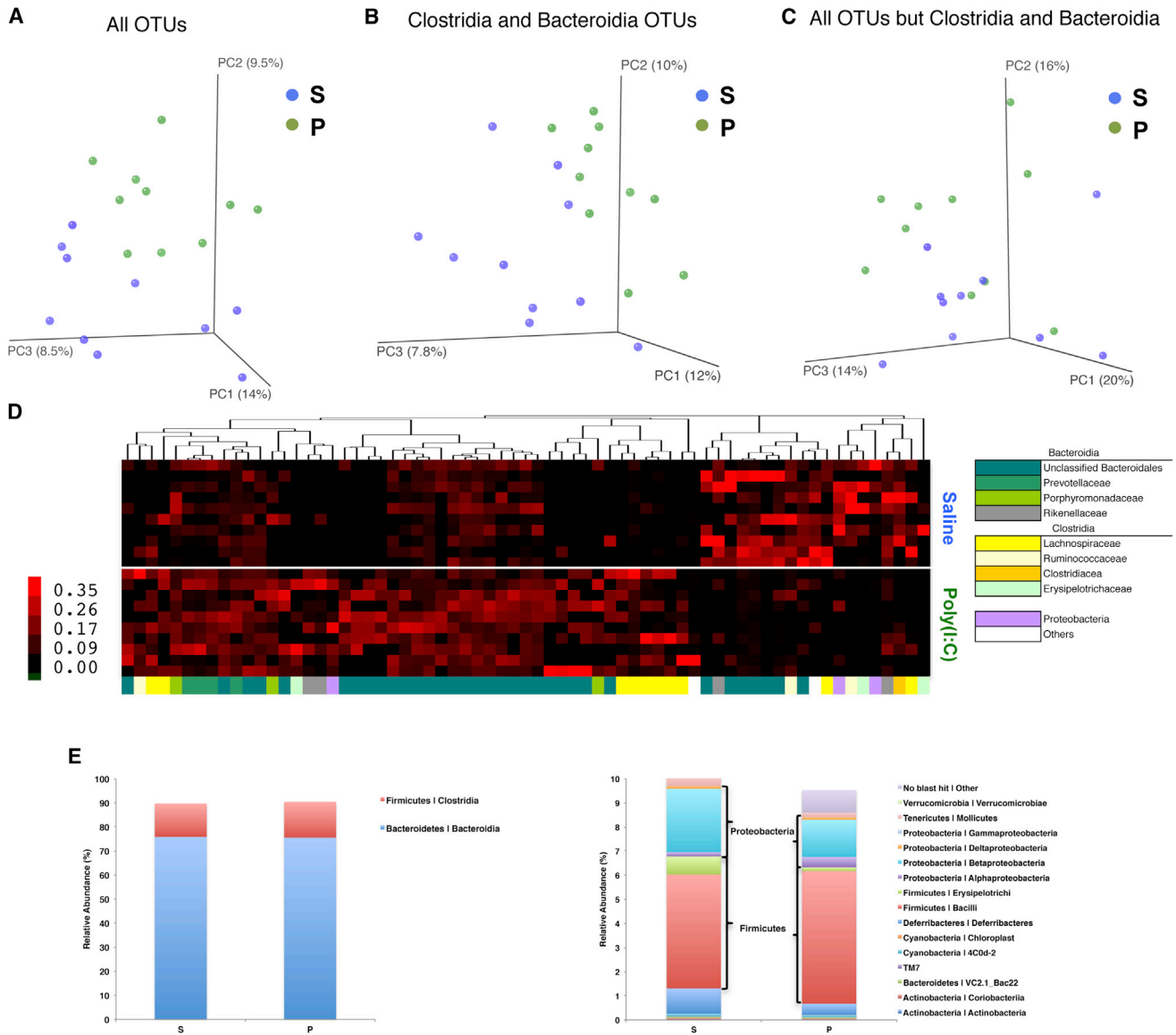


Figure 2. MIA Offspring Exhibit Dysbiosis of the Intestinal Microbiota

(A) Unweighted UniFrac-based 3D PCoA plot based on all OTUs from feces of adult saline+vehicle (S) and poly(I:C)+vehicle (P) offspring. (B) Unweighted UniFrac-based 3D PCoA plot based on subsampling of Clostridia and Bacteroidia OTUs (2003 reads per sample). (C) Unweighted UniFrac-based 3D PCoA plot based on subsampling of OTUs remaining after subtraction of Clostridia and Bacteroidia OTUs (47 reads per sample). (D) Relative abundance of unique OTUs of the gut microbiota (bottom, x axis) for individual biological replicates (right, y axis), where red hues denote increasing relative abundance of a unique OTU. (E) Mean relative abundance of OTUs classified at the class level for the most (left) and least (right) abundant taxa. n = 10/group. Data were simultaneously collected and analyzed for poly(I:C)+*B. fragilis* treatment group (See Figure 4). See also Figure S2 and Table S1.

MIA offspring (Figures 1D and S1C), but these are not affected by *B. fragilis* treatment, revealing specificity for IL-6. We further find that recombinant IL-6 treatment can modulate colon levels of both CLDN 8 and 15 in vivo and in vitro colon organ cultures (data not shown), suggesting that *B. fragilis*-mediated restoration of colonic IL-6 levels could underlie its effects on gut permeability. Collectively, these findings demonstrate that *B. fragilis* treatment of MIA offspring improves defects in GI

barrier integrity and corrects alterations in tight junction and cytokine expression.

***B. fragilis* Treatment Restores Specific Microbiota Changes in MIA Offspring**

The finding that *B. fragilis* ameliorates GI defects in MIA offspring prompted us to examine its effects on the intestinal microbiota. No significant differences are observed following

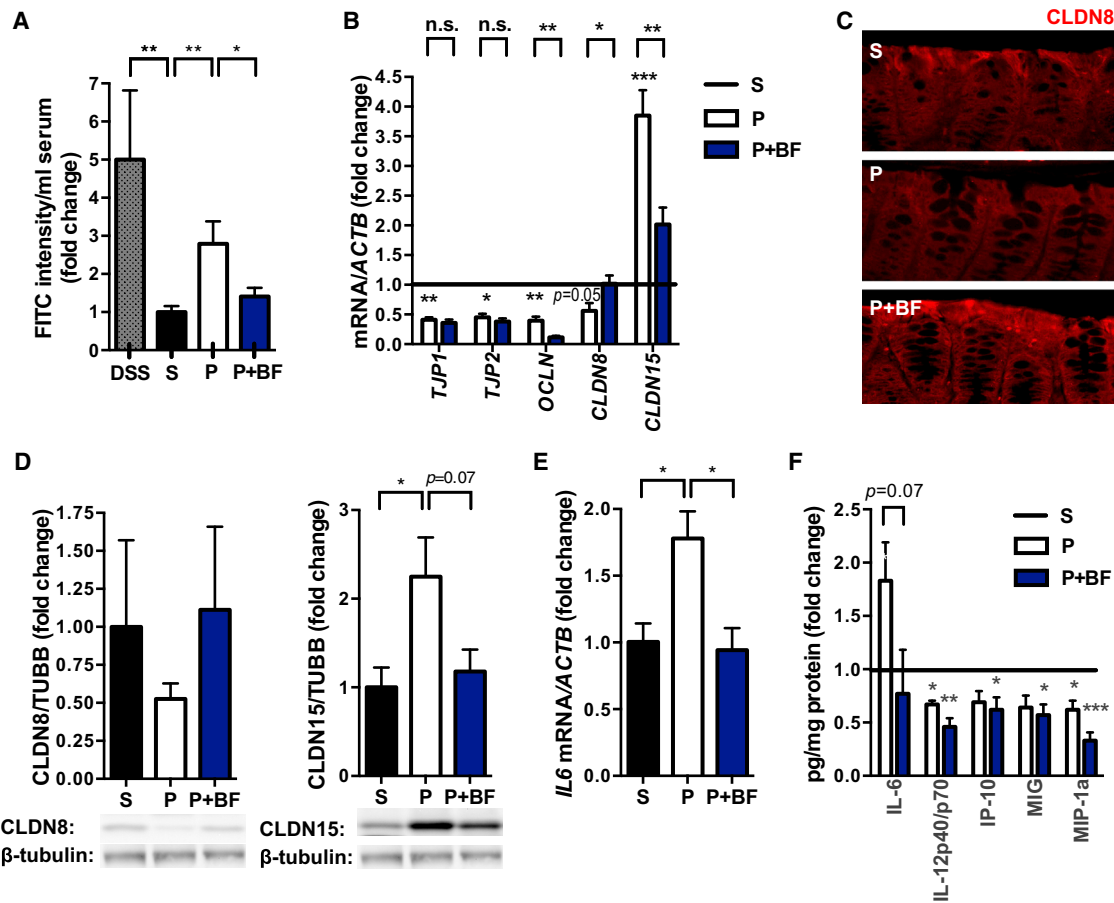


Figure 3. *B. fragilis* Treatment Corrects GI Deficits in MIA Offspring

(A) Intestinal permeability assay, measuring FITC intensity in serum after oral gavage of FITC-dextran. Data are normalized to saline controls. Data for DSS, saline + vehicle (S) and poly(I:C) + vehicle (P) are as in Figure 1. poly(I:C)+*B. fragilis* (P+BF): n = 9/group.
 (B) Colon expression of tight junction components relative to β -actin. Data for each gene are normalized saline controls. Data for S and P are as in Figure 1. Asterisks directly above bars indicate significance compared to saline control (normalized to 1, as denoted by the black line), whereas asterisks at the top of the graph denote statistical significance between P and P+BF groups. n = 8/group.
 (C) Immunofluorescence staining for claudin 8. Representative images for n = 5.
 (D) Colon protein levels of claudin 8 (left) and claudin 15 (right). Representative signals are depicted below. Data are normalized to signal intensity in saline controls. n = 3/group.
 (E) Colon expression of IL-6 relative to β -actin. Data are normalized to saline controls. Data for S and P are as in Figure 1. P+BF: n = 3/group.
 (F) Colon protein levels of cytokines and chemokines relative to total protein content. Data are normalized to saline controls. Data for S and P are as in Figure 1. n = 10/group.
 See also Figure S1.

B. fragilis treatment of MIA offspring by PCoA (ANOSIM R = 0.0060 p = 0.4470; Table S3), in microbiota richness (PD: p = 0.2980, Observed Species: p = 0.5440) and evenness (Gini: p = 0.6110, Simpson Evenness: p = 0.5600; Figures 4A, S2A and S2B), or in relative abundance at the class level (Figure S2C). However, evaluation of key OTUs that discriminate adult MIA offspring from controls reveals that *B. fragilis* treatment significantly alters levels of 35 OTUs (Table S2). Specifically, MIA offspring treated with *B. fragilis* display significant restoration in the relative abundance of 6 out of the 67 OTUs found to discriminate MIA from control offspring (Figure 4B and Table S2), which are taxonomically assigned as unclassified Bacteroidia and Clostridia of the family *Lachnospiraceae* (Figure 4B and Table S2). Notably, these alterations occur in

the absence of persistent colonization of *B. fragilis*, which remains undetectable in fecal and cecal samples isolated from treated MIA offspring (Figures S2D and S2E). Phylogenetic reconstruction of the OTUs that are altered by MIA and restored by *B. fragilis* treatment reveals that the Bacteroidia OTUs cluster together into a monophyletic group and the *Lachnospiraceae* OTUs cluster into two monophyletic groups (Figure 4C). This result suggests that, although treatment of MIA offspring with *B. fragilis* may not lead to persistent colonization, this probiotic corrects the relative abundance of specific groups of related microbes of the *Lachnospiraceae* family as well as unclassified Bacteroidales. Altogether, we demonstrate that treatment of MIA offspring with *B. fragilis* ameliorates particular MIA-associated alterations in the commensal microbiota.

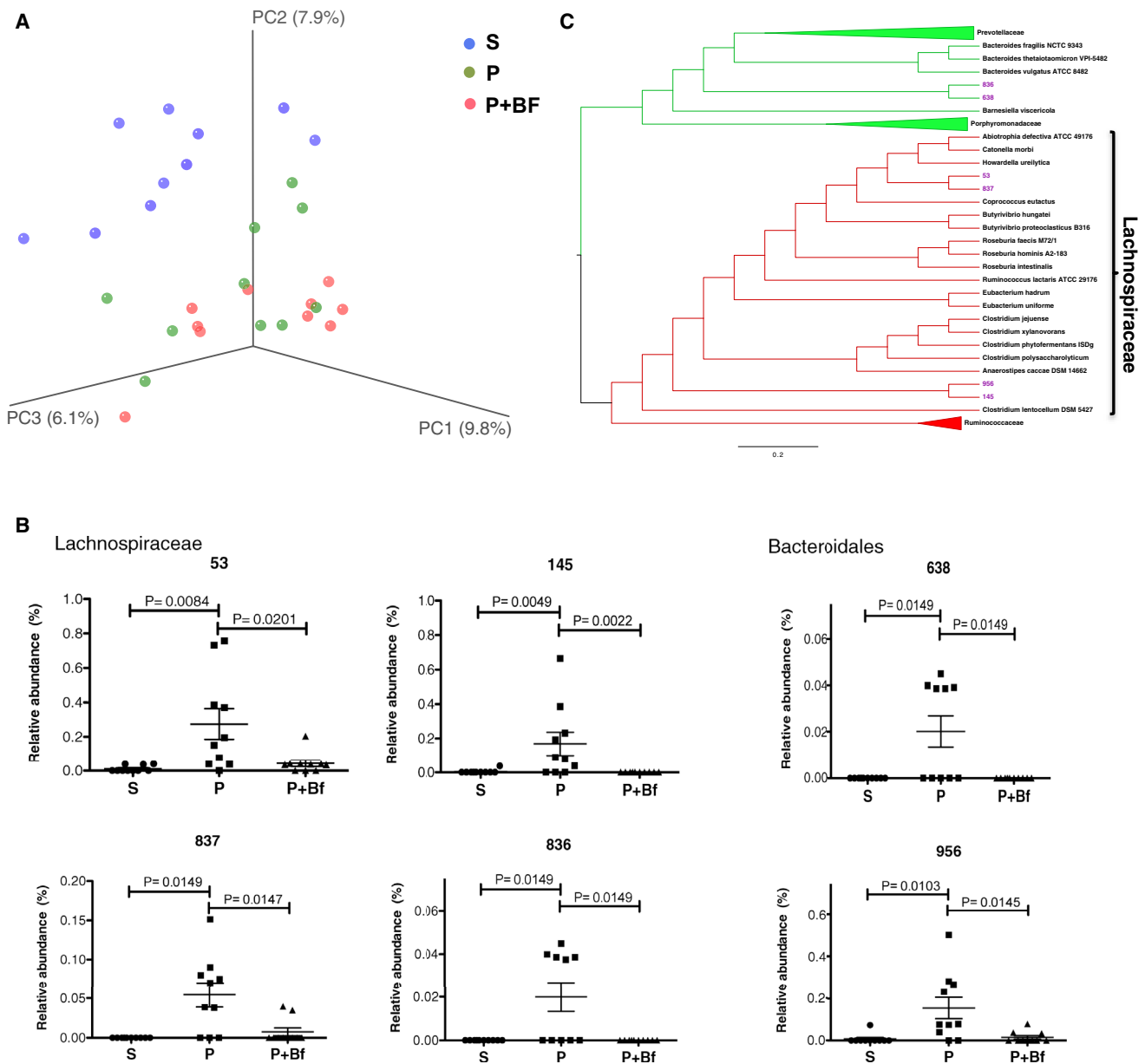


Figure 4. *B. fragilis* Treatment Alters the Intestinal Microbiota and Corrects Species-Level Abnormalities in MIA Offspring

(A) Unweighted UniFrac-based 3D PCoA plot based on all OTUs. Data for saline (S) and poly(I:C) (P) are as in Figure 2.

(B) Relative abundance of key OTUs of the family *Lachnospiraceae* (top) and order *Bacteroidales* (bottom) that are significantly altered by MIA and restored by *B. fragilis* treatment.

(C) Phylogenetic tree based on nearest-neighbor analysis of 16S rRNA gene sequences for key OTUs presented in (B). Red clades indicate OTUs of the family *Lachnospiraceae* and green clades indicate OTUs of the order *Bacteroidales*. Purple taxa indicate OTUs that are significantly elevated in P and corrected by *B. fragilis* (BF) treatment. n = 10/group.

See also Figure S2 and Table S2.

***B. fragilis* Treatment Corrects ASD-Related Behavioral Abnormalities**

Studies suggest that GI issues can contribute to the development, persistence, and/or severity of symptoms seen in ASD and related neurodevelopmental disorders (Buie et al., 2010; Coury et al., 2012). To explore the potential impact of GI dysfunction on core ASD behavioral abnormalities, we tested whether

B. fragilis treatment impacts anxiety-like, sensorimotor, repetitive, communicative, and social behavior in MIA offspring. We replicated previous findings that adult MIA offspring display several core behavioral features of ASD (Malkova et al., 2012). Open field exploration involves mapping an animal's movement in an open arena to measure locomotion and anxiety (Bourin et al., 2007). MIA offspring display decreased entries and time

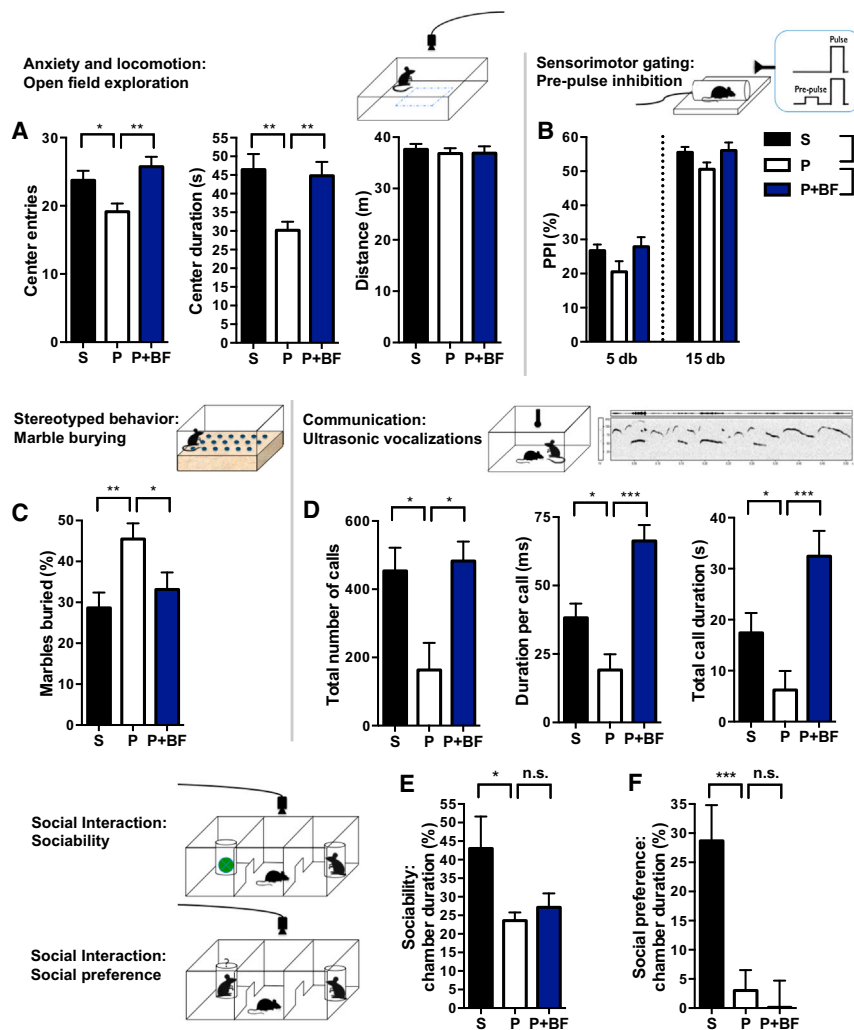


Figure 5. *B. fragilis* Treatment Ameliorates Autism-Related Behavioral Abnormalities in MIA Offspring

(A) Anxiety-like and locomotor behavior in the open field exploration assay. $n = 35\text{--}75/\text{group}$. (B) Sensorimotor gating in the PPI assay. $n = 35\text{--}75/\text{group}$. (C) Repetitive marble burying assay. $n = 16\text{--}45/\text{group}$. (D) Ultrasonic vocalizations produced by adult male mice during social encounter. $n = 10/\text{group}$. S = saline+vehicle, p = poly(I:C)+vehicle, P+BF = poly(I:C)+*B. fragilis*. Data were collected simultaneously for poly(I:C)+*B. fragilis* Δ PSA and poly(I:C)+*B. thetaiotaomicron* treatment groups (See also Figures S3 and S4).

related impairments in social interaction (Silverman et al., 2010). MIA offspring exhibit deficits in both sociability, or preference to interact with a novel mouse over a novel object, and social preference (social novelty), or preference to interact with an unfamiliar versus a familiar mouse (Figures 5E and 5F). Altogether, MIA offspring demonstrate a number of behavioral abnormalities associated with ASD as well as others such as anxiety and deficient sensorimotor gating.

Remarkably, oral treatment with *B. fragilis* ameliorates many of these behaviors. *B. fragilis*-treated MIA offspring do not exhibit anxiety-like behavior in the open field (Figure 5A; compare poly(I:C) [P] to poly(I:C)+*B. fragilis* [P+BF]), as shown by restoration in the number of center entries and duration of time spent in the center of the arena. *B. fragilis* improves sensorimotor gating in MIA offspring, as indicated by increased combined PPI in response to 5 and 15 db prepulses (Figure 5B), with no significant effect on the intensity of startle to the acoustic stimulus (data not shown). *B. fragilis*-treated mice also exhibit decreased levels of stereotyped marble burying and restored communicative behavior (Figures 5C and 5D). Interestingly, *B. fragilis* raises the duration per call by MIA offspring to levels exceeding those observed in saline controls (Figure 5D), suggesting that despite normalization of the propensity to communicate (number of calls), there is a qualitative difference in the types of calls generated with enrichment of longer syllables.

Although *B. fragilis*-treated MIA offspring exhibit improved communicative, repetitive, anxiety-like, and sensorimotor behavior, they retain deficits in sociability and social preference (Figure 5E). Selective amelioration of ASD-related behaviors is also seen with risperidone treatment of CNTNAP2 knockout mice, a genetic mouse model for ASD (Peñagarikano et al., 2011), wherein communicative and repetitive, but not social, behavior is corrected. These data suggest that there may be

spent in the center of the arena, which is indicative of anxiety-like behavior (Figure 5A; compare saline [S] to poly(I:C) [P]). The prepulse inhibition (PPI) task measures the ability of an animal to inhibit its startle in response to an acoustic tone (“pulse”) when it is preceded by a lower-intensity stimulus (“prepulse”). Deficiencies in PPI are a measure of impaired sensorimotor gating and are observed in several neurodevelopmental disorders, including autism (Perry et al., 2007). MIA offspring exhibit decreased PPI in response to 5 or 15 db prepulses (Figure 5B). The marble burying test measures the propensity of mice to engage repetitively in a natural digging behavior that is not confounded by anxiety (Thomas et al., 2009). MIA offspring display increased stereotyped marble burying compared to controls (Figure 5C). Ultrasonic vocalizations are used to measure communication by mice, wherein calls of varying types and motifs are produced in different social paradigms (Grimsley et al., 2011). MIA offspring exhibit deficits in communication, as indicated by reduced number and duration of ultrasonic vocalizations produced in response to a social encounter (Figure 5D). Finally, the three-chamber social test is used to measure ASD-

improves sensorimotor gating in MIA offspring, as indicated by increased combined PPI in response to 5 and 15 db prepulses (Figure 5B), with no significant effect on the intensity of startle to the acoustic stimulus (data not shown). *B. fragilis*-treated mice also exhibit decreased levels of stereotyped marble burying and restored communicative behavior (Figures 5C and 5D). Interestingly, *B. fragilis* raises the duration per call by MIA offspring to levels exceeding those observed in saline controls (Figure 5D), suggesting that despite normalization of the propensity to communicate (number of calls), there is a qualitative difference in the types of calls generated with enrichment of longer syllables.

Although *B. fragilis*-treated MIA offspring exhibit improved communicative, repetitive, anxiety-like, and sensorimotor behavior, they retain deficits in sociability and social preference (Figure 5E). Selective amelioration of ASD-related behaviors is also seen with risperidone treatment of CNTNAP2 knockout mice, a genetic mouse model for ASD (Peñagarikano et al., 2011), wherein communicative and repetitive, but not social, behavior is corrected. These data suggest that there may be

differences in the circuitry or circuit plasticity governing social behavior as compared to the other behaviors and that *B. fragilis* treatment may modulate specific circuits during amelioration of at least some ASD and possibly other neurodevelopmental behavioral defects.

Interestingly, behavioral improvement in response to *B. fragilis* treatment of MIA offspring is not associated with changes in systemic immunity (Figures S3A–S3D) and is not dependent on polysaccharide A (PSA), a molecule previously identified to confer immunomodulatory effects by *B. fragilis* (Figure S3E) (Mazmanian et al., 2008; Ochoa-Repáraz et al., 2010; Round and Mazmanian, 2010). Furthermore, amelioration of behavior is not specific to *B. fragilis*, as similar treatment with *Bacteroides thetaiotaomicron* also significantly improves anxiety-like, repetitive, and communicative behavior in MIA offspring (Figure S4). This is consistent with our finding that *B. fragilis* treatment improves behavioral problems in the absence of evident colonization of *B. fragilis* in the GI tract (Figures S2D and S2E) and thus may be functioning through persistent shifts in the composition of resident microbiota (Figure 4). There is, however, some degree of specificity to bacterial treatment, as administration of *Enterococcus faecalis* has no effect on anxiety-like and repetitive behavior in MIA offspring (data not shown).

The Serum Metabolome is Modulated by MIA and *B. fragilis* Treatment

Metabolomic studies have shown that gut microbial products are found in many extraintestinal tissues, and molecules derived from the microbiota may influence metabolic, immunologic, and behavioral phenotypes in mice and humans (Blumberg and Powrie, 2012; Nicholson et al., 2012). Given that MIA offspring display increased gut permeability, tight junction defects, and dysbiosis, we hypothesized that gut bacteria may affect the metabolome of mice. We utilized gas chromatography/liquid chromatography with mass spectrometry (GC/LC-MS)-based metabolomic profiling to identify MIA-associated changes in serum metabolites. Three hundred and twenty-two metabolites were detected in sera from adult mice (Table S5). Interestingly, MIA leads to statistically significant alterations in 8% of all serum metabolites detected (Table S4). Furthermore, postnatal *B. fragilis* treatment has a significant effect on the serum metabolome, altering 34% of all metabolites detected (Table S5 and Figure S5).

B. fragilis Treatment Corrects Levels of MIA-Induced Serum Metabolites

Consistent with the notion that increased intestinal permeability leads to leakage of gut-derived metabolites into the bloodstream, we hypothesized that *B. fragilis*-mediated improvement of intestinal barrier integrity would restore serum levels of certain metabolites. We therefore focused on serum metabolites that are significantly altered by MIA treatment and restored to control levels by *B. fragilis* treatment. The most dramatically affected metabolite is 4-ethylphenylsulfate (4EPS), displaying a striking 46-fold increase in serum levels of MIA offspring that is completely restored by *B. fragilis* treatment (Figure 6A). This metabolite is of particular interest because of the reported production of 4EPS by GI microbes and proposed role for

4EPS in communication by mice (Lafaye et al., 2004). Moreover, we find that compared to conventionally colonized (SPF [specific pathogen free]) mice, germ-free (GF) mice display nearly undetectable levels of serum 4EPS, indicating that serum 4EPS is derived from, or modulated by, the commensal microbiota (Figure 6B). Interestingly, 4EPS is suggested to be a uremic toxin, as is *p*-cresol (4-methylphenol), a chemically related metabolite reported to be a possible urinary biomarker for autism (Altieri et al., 2011; Persico and Napolioni, 2013). MIA offspring also exhibit elevated levels of serum *p*-cresol, although the increase does not reach statistical significance (Table S5). The fact that 4EPS shares close structural similarity to the toxic sulfated form of *p*-cresol (4-methylphenylsulfate; 4MPS) is intriguing as the two metabolites may exhibit functional overlap (Figure S6A).

In addition to 4EPS, MIA offspring display significantly increased levels of serum indolepyruvate, a key molecule of the tryptophan metabolism pathway, which is restored to control levels by *B. fragilis* treatment (Figure 6A). Indolepyruvate is generated by tryptophan catabolism and, like 4EPS, is believed to be produced by gut microbes (Smith and Macfarlane, 1997) (Figure S6B). MIA offspring also exhibit increased levels of serum serotonin ($0.05 < p < 0.10$; Tables S3 and S4), reflecting another alteration in tryptophan metabolism, analogous to the well-established hyperserotonemia endophenotype of autism. MIA also leads to altered serum glycolate, imidazole propionate, and N-acetylserine levels (Figure 6A), which are corrected by *B. fragilis* treatment. How changes in these metabolites may be relevant to ASD or GI dysfunction is currently unknown but may be an exciting area for future study. These findings demonstrate that specific metabolites are altered in MIA offspring and normalized by *B. fragilis* treatment, with at least two molecules (4EPS and indolepyruvate) having potential relevance to ASD.

A Serum Metabolite Induces Anxiety-like Behavior

Do small molecules modulated by the commensal microbiota play a role in behaviors relevant to ASD? To test this hypothesis, we examined whether increasing serum 4EPS is sufficient to cause any ASD-related behavioral abnormalities in naive mice. Mice were treated with 4EPS potassium salt (Figures S7A–S7C) or vehicle, daily from 3 weeks of age (when MIA offspring display gut permeability) to 6 weeks of age (when behavior testing begins). Remarkably, systemic administration of the single metabolite, 4EPS, to naive wild-type mice is sufficient to induce anxiety-like behavior similar to that observed in MIA offspring (Figure 6C). Relative to vehicle-treated controls, mice exposed to 4EPS travel comparable distances in the open field but spend less time in the center arena (Figure 6C). Also, in the PPI test, 4EPS-treated mice exhibit increased intensity of startle in response to the unconditioned primary stimulus but no significant alterations in PPI (Figure 6D), representing anxiety-associated potentiation of the startle reflex (Bourin et al., 2007). Interestingly, vehicle-treated controls exhibit symptoms of anxiety-like behavior compared to untreated saline offspring (vehicle vs saline in Figure 6C and 5A), reflecting the well-known effect of chronic stress (daily injection) on raising anxiety levels in mice. Conversely, there are no significant differences between 4EPS-treated versus saline-treated mice in marble burying or

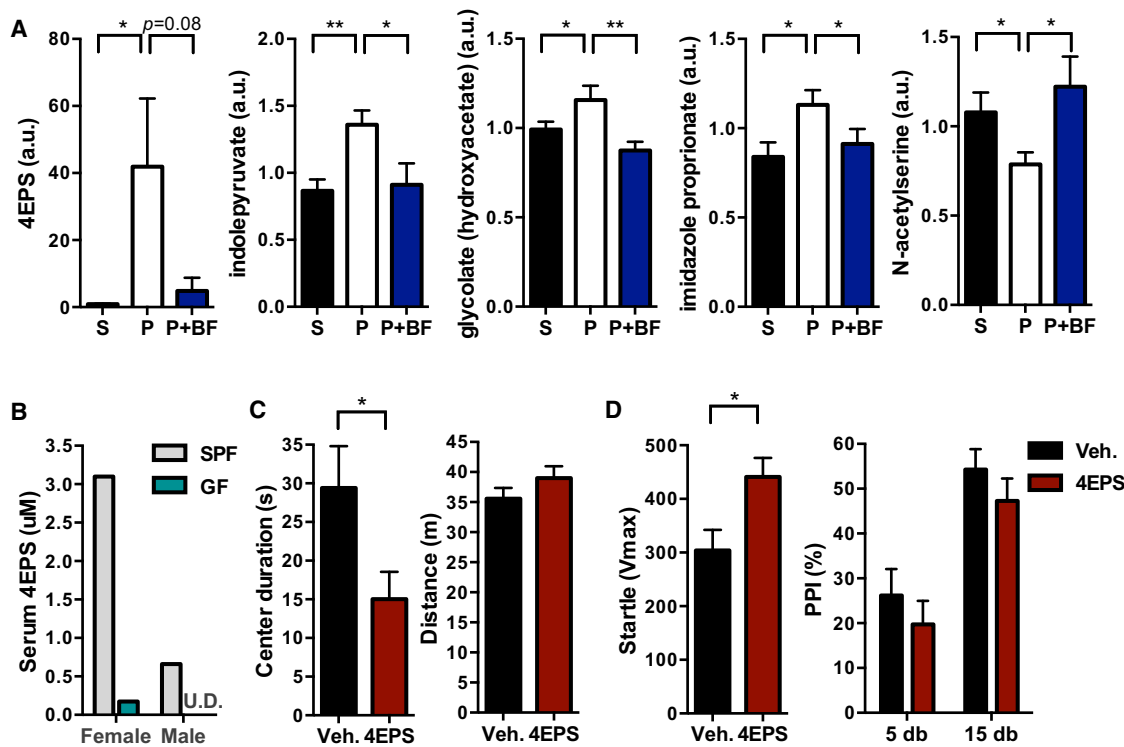


Figure 6. *B. fragilis* Treatment Corrects MIA-Mediated Changes in 4-ethylphenylsulfate, a Microbe-Dependent Metabolite that Induces Anxiety-like Behavior

(A) Relative quantification of metabolites detected by GC/LC-MS that are significantly altered by MIA and restored by *B. fragilis* treatment. $n = 8$ /group.

(B) Serum concentrations of 4EPS detected by LC-MS. $n = 1$, where each represents pooled sera from 3–5 mice.

(C) Anxiety-like and locomotor behavior in the open field exploration assay. $n = 10$ /group.

(D) Potentiated startle reflex in the PPI assay. $n = 10$ /group.

S = saline+vehicle, P = poly(I:C)+vehicle, P+BF = poly(I:C)+*B. fragilis*, SPF = specific pathogen-free (conventionally-colonized), GF = germ-free, Veh. = vehicle (saline), 4EPS = 4-ethylphenylsulfate. U.D. = undetectable. See also Figures S5, S6, and S7 and Tables S3 and S4.

USV behavior (Figures S7D and S7E), suggesting that elevating serum 4EPS levels specifically promotes anxiety-like behavior. While not a core diagnostic criterion, anxiety is a common comorbidity that may contribute to cardinal ASD symptoms. Furthermore, it is possible that complex behaviors may be modulated by combinations of metabolites. In summary, these data reveal that elevated systemic levels of a metabolite regulated by gut microbes causes anxiety-like behavior, suggesting that molecular connections between the gut and the brain may be associated with specific symptoms relevant to ASD and other neurodevelopmental disorders.

DISCUSSION

We demonstrate that the MIA mouse model displays behavioral symptoms relevant to ASD and other neurodevelopmental disorders (Malkova et al., 2012; Shi et al., 2009), while also exhibiting defective GI integrity, dysbiosis of the commensal microbiota, and alterations in serum metabolites. At least some of these alterations are similar to endophenotypes observed in subsets of ASD individuals. Increased intestinal permeability (Boukthir et al., 2010; D'Eufemia et al., 1996; de Magistris et al., 2010) and microbiome alterations (Adams et al., 2011; Finegold

et al., 2010; Finegold et al., 2012; Kang et al., 2013; Parracho et al., 2005; Williams et al., 2011; Williams et al., 2012) are reported in several independent studies of ASD; however, these findings are challenged by some reports of no significant differences between cases and controls (Gondalia et al., 2012; Robertson et al., 2008). The reported prevalence of GI abnormalities in ASD also varies considerably across studies, ranging from 9%–91%. Many such investigations have methodological limitations, including inappropriate experimental controls, high sample heterogeneity, small sample size, and selection bias. In addition, the definition and assessment of GI symptoms can differ across studies, contributing to variation. While a number of studies support a role for GI complications in ASD, additional prospective population-based studies are needed to evaluate the frequency of GI symptoms in ASD and the interesting possibility that GI conditions are enriched in particular ASD subtypes. The role of GI abnormalities and their contribution to symptoms in other neurodevelopmental disorders warrants further investigation as well.

We find that treatment with *B. fragilis* corrects intestinal permeability defects, as well as altered levels of tight junction proteins and cytokines in mice displaying GI and neurological symptoms related to ASD. The ability of *B. fragilis* to selectively

ameliorate MIA-associated increases in colon IL-6 is interesting as this cytokine is required for the development of behavioral deficits in MIA offspring (Smith et al., 2007). Many cytokines including IL-6 regulate tight junction expression and intestinal barrier integrity, and further, a variety of enteric microbes are known to regulate intestinal tight junction and cytokine levels (Turner, 2009). Our study suggests that *B. fragilis* is able to ameliorate leaky gut by directly targeting tight junction expression, cytokine production, and/or microbiome composition. Intriguingly, a recent analysis in humans showed that among the Bacteroidaceae family, only a single phylotype most closely related to *B. fragilis* was selectively depleted in ASD children compared to matched controls, and most dramatically in those subjects with more severe GI issues (D.-W. Kang and R. Krajmalnik-Brown, personal communication). Thus, the correlation between *B. fragilis* and improved intestinal health is present in both mice and humans.

Consistent with the role of GI microbes in regulating intestinal permeability and metabolic homeostasis (Nicholson et al., 2012; Wikoff et al., 2009), we show that *B. fragilis* treatment corrects MIA-associated changes in specific serum metabolites that appear to have a gut origin, suggesting *B. fragilis* may prevent leakage of harmful molecules from the GI lumen. In a proof-of-concept test of this hypothesis, we reveal that the microbially-modulated metabolite 4EPS, which is elevated in the circulation by MIA and restored by *B. fragilis* treatment, is sufficient to induce anxiety-like behavior in naive mice. These data indicate that metabolic changes contribute to the onset and/or persistence of autism-related behavioral abnormalities. Notably, we show that commensal microbes are required for the production of serum 4EPS in mice. Several species of *Clostridium* are believed to be producers of the precursor 4-ethylphenol (Nicholson et al., 2012), consistent with our findings that levels of the *Lachnospiraceae* family of Clostridia and serum 4EPS are elevated in MIA offspring, and both are corrected by *B. fragilis* treatment. Moreover, the structural similarity of 4EPS to the putative ASD biomarker p-cresol, which also derives from *Clostridium* species (Persico and Napolioni, 2013), suggests they may be produced through similar biosynthetic pathways (see Figure S6A). Similarly, the elevation in serum indolepyruvate observed in MIA offspring, which is also corrected by *B. fragilis* treatment, is reminiscent of reported increases in indolyl-3-acryloylglycine (IAG) in human ASD (Bull et al., 2003), which is involved in GI homeostasis and produced by bacterial metabolism (Keszthelyi et al., 2009). Although not all autism-like behaviors are affected by 4EPS alone, our results warrant the examination of indolepyruvate and several other serum metabolites, perhaps in combination, for their potential to impact the spectrum of behaviors relevant to neurodevelopmental disorders.

Remarkably, *B. fragilis* treatment ameliorates abnormal communicative, stereotyped, sensorimotor and anxiety-like behaviors in MIA offspring, supporting emerging evidence for a gut-brain link in modulating neurodevelopmental disorders. A role for commensal bacteria in modulating behavior is supported by studies revealing differences between GF and SPF mice in anxiety-like (Diaz Heijtz et al., 2011), nociceptive (Amaral et al., 2008) and social behavior (Desbonnet et al., 2013). GF mice

also exhibit widespread microbiota-dependent changes in brain gene expression, in pathways relevant to synaptic function and long-term potentiation (Diaz Heijtz et al., 2011). Furthermore, microbial treatment can ameliorate depressive (Bravo et al., 2011) and anxiety-like behavior (Bercik et al., 2011) in SPF mice, and probiotic treatment has been beneficial in treating psychological distress and chronic fatigue symptoms in humans (Messaoudi et al., 2011; Rao et al., 2009). The molecular mechanisms underlying how the microbiota regulates brain activity and behavior are unclear but could be mediated by vagus nerve innervation, immunomodulation and/or metabolic signaling.

Our findings provide a mechanism by which a human commensal bacterium can improve ASD-related GI deficits and behavioral abnormalities in mice. Importantly, particular behavioral and neuropathological symptoms seen in the MIA model (and in human autism) are not exclusive to ASD. MIA offspring exhibit additional endophenotypes that resemble schizophrenia, such as enlarged ventricles, deficient latent inhibition and deficient parvalbumin-positive interneurons (Li et al., 2009; Smith et al., 2007), and the behavioral abnormalities characteristic to human ASD can be individually seen in other neurological diseases such as schizophrenia, obsessive compulsive disorder, Angelman syndrome, and Prader-Willi syndrome. Moreover, other nondiagnostic behaviors relevant to ASD, including anxiety and impaired PPI, are commonly reported in several neurological disorders. The phenotypic overlaps across different disease diagnoses suggest that our findings on the gut-microbiome-brain connection and microbe-based treatments for behavior might be broadly applicable to various disorders. We propose the transformative concept that autism, and likely other behavioral conditions, are potentially diseases involving the gut that ultimately impact the immune, metabolic, and nervous systems, and that microbiome-mediated therapies may be a safe and effective treatment for these neurodevelopmental disorders.

EXPERIMENTAL PROCEDURES

See [Supplemental Information](#) for additional details and references.

Animals and MIA

Pregnant C57BL/6N mice (Charles River; Wilmington, MA) were injected i.p. on E12.5 with saline or 20 mg/kg poly(I:C) according to methods described in Smith et al. (2007). All animal experiments were approved by the Caltech IACUC.

B. fragilis Treatment

Mice were selected at random for treatment with *B. fragilis* NCTC 9343 or vehicle, every other day for 6 days at weaning. 10^{10} CFU of freshly grown *B. fragilis*, or vehicle, in 1.5% sodium bicarbonate was administered in sugar-free applesauce over standard food pellets. The same procedure was used for mutant *B. fragilis* PSA and *B. thetaiotaomicron*.

Intestinal Permeability Assay

Mice were fasted for 4 hr before gavage with 0.6 g/kg 4 kDa FITC-dextran (Sigma Aldrich). Four hours later, serum samples were read for fluorescence intensity at 521 nm using an xFluor4 spectrometer (Tecan). Mice were fed 3% dextran sulfate sodium salt (DSS; MP Biomedicals) in drinking water for 7 days to induce colitis.

16S rRNA Gene Sequence Analysis

16S data were processed and its diversity was analyzed using QIIME 1.6 software package (Caporaso et al., 2010b). OTUs were assigned taxonomic classification using the basic BLAST classifier (Altschul et al., 1990). For tree-based alpha- and beta diversity analyses, representative sequences for each OTU were aligned using PyNAST (Caporaso et al., 2010a) and a phylogenetic tree was constructed based on this alignment using FastTree (Price et al., 2009). Beta diversity was assessed from unweighted UniFrac, using the analysis of similarity (ANOSIM; Fierer et al., 2010), permutational multivariate analysis of variance (PERMANOVA; Anderson, 2008), permutational analysis of multivariate dispersions (PERMDISP; Anderson et al., 2006), and Moran's I.

Identification of Differences in Specific OTUs

Key OTUs were identified using: (1) Metastats comparison (White et al., 2009) and (2) Random Forests algorithm, under QIIME (Knights et al., 2011) or coupled with Boruta feature selection, in the Genboree microbiome toolset (Riehle et al., 2012), and (3) Galaxy platform-based LDA Effect Size analysis (LEFSe; Segata et al., 2011). Key OTUs were then aligned using the SINA aligner (<http://www.arb-silva.de/aligner/>; Pruesse et al., 2012), compared to the SILVA reference database release 111 (Quast et al., 2013) using Arb (Ludwig et al., 2004) and visualized using FigTree (<http://tree.bio.ed.ac.uk/software/figtree/>). Heat maps of key OTUs were generated by extracting their relative abundance from the OTU table and clustering data by correlation using Cluster 3.0 (de Hoon et al., 2004). Abundance data were visualized using Java TreeView (Saldanha, 2004) (Data Set S1).

Behavioral Testing

MIA and control offspring were behaviorally tested as in Hsiao et al. (2012) and Malkova et al. (2012). Mice were tested beginning at 6 weeks of age for PPI, open field exploration, marble burying, social interaction, and adult ultrasonic vocalizations.

4EPS Sufficiency Experiments

Wild-type mice were injected i.p. with saline or 30 mg/kg 4EPS potassium salt daily from 3 to 6 weeks of age. A dose-response curve was generated by measuring serum 4EPS levels at various times after i.p. injection of 30 mg/kg 4EPS (Figure S7C). Mice were behaviorally tested as described above from 6 to 9 weeks of age.

Statistical Analysis

Statistical analysis was performed using Prism software (Graphpad). Data are plotted in the figures as mean \pm SEM. Differences between two treatment groups were assessed using two-tailed, unpaired Student's *t* test with Welch's correction. Differences among three or more groups were assessed using one-way ANOVA with Bonferroni post hoc test. Two-way repeated-measures ANOVA with Bonferroni post hoc test was used for analysis of PPI and CD4+ T cell stimulation data. Two-way ANOVA with contrasts was used for analysis of the metabolite data. Significant differences are indicated in the figures by * $p < 0.05$, ** $p < 0.01$, *** $p < 0.001$. Notable near-significant differences ($0.5 < p < 0.1$) are indicated in the figures. Notable nonsignificant (and nonnear significant) differences are indicated in the figures by "n.s."

SUPPLEMENTAL INFORMATION

Supplemental Information includes Extended Experimental Procedures, seven figures, five tables, and one data set and can be found with this article online at <http://dx.doi.org/10.1016/j.cell.2013.11.024>.

AUTHOR CONTRIBUTIONS

E.Y.H., P.H.P. and S.K.M. designed the study, E.Y.H., S.W.M., S.H., J.A.C. and J.C. performed the experiments and analyzed the data, E.R.H., T.M., G.S. and J.F.P. conducted microbiota sequencing and analysis, S.E.R. contributed novel reagents, E.Y.H., S.W.M., G.S., J.A.C., P.H.P. and S.K.M. wrote the

manuscript. All authors discussed the results and commented on the manuscript.

ACKNOWLEDGMENTS

We acknowledge Reyna Sauza, Jaime Rodriguez, and Taren Thron for caring for the animals; Dr. Michael Fischbach (UCSF) for advising on pathways of 4EPS and indolepyruvate synthesis; Dr. Nadim Ajami (Baylor) for providing helpful comments on the manuscript; Greg Donaldson (Caltech) for conducting experiments on microbial viability; Dr. Kym Faull (UCLA) for conducting pilot GC/MS experiments; Dr. Alessio Fasano (Massachusetts General) for conducting pilot microbiota sequencing experiments; and Dr. Jerrold Turner (U Chicago) for providing histological analysis of intestinal sections. This work was supported by a Caltech Innovation Fellowship (to E.Y.H.), Autism Speaks Weatherstone Fellowship (to E.Y.H.), NIH/NRSA Predoctoral Fellowship (to E.Y.H.), Human Frontiers Science Program Fellowship (to G.S.), DOD Graduate Fellowship (to J.A.C.), NSF Graduate Research Fellowship (to J.A.C.), Autism Speaks Trailblazer Award (to P.H.P. and S.K.M.), Caltech Innovation Initiative (to P.H.P. and S.K.M.), Caltech Grubstake Awards (to P.H.P. and S.K.M.), Congressionally Directed Medical Research Award (to P.H.P. and S.K.M.), Weston Havens Award (to P.H.P. and S.K.M.), Callie D. McGrath Charitable Foundation awards (to P.H.P.) and NIMH grant MH100556 (to P.H.P. and S.K.M.).

Received: August 20, 2013

Revised: October 3, 2013

Accepted: November 18, 2013

Published: December 5, 2013

REFERENCES

- Abdallah, M.W., Larsen, N., Grove, J., Nørgaard-Pedersen, B., Thorsen, P., Mortensen, E.L., and Hougaard, D.M. (2013). Amniotic fluid inflammatory cytokines: potential markers of immunologic dysfunction in autism spectrum disorders. *World J. Biol. Psychiatry* 14, 528–538.
- Adams, J.B., Johansen, L.J., Powell, L.D., Quig, D., and Rubin, R.A. (2011). Gastrointestinal flora and gastrointestinal status in children with autism—comparisons to typical children and correlation with autism severity. *BMC Gastroenterol.* 11, 22.
- Altieri, L., Neri, C., Sacco, R., Curatolo, P., Benvenuto, A., Mura, F., Santocchi, E., Bravaccio, C., Lenti, C., Saccani, M., et al. (2011). Urinary p-cresol is elevated in small children with severe autism spectrum disorder. *Biomarkers* 16, 252–260.
- Altschul, S.F., Gish, W., Miller, W., Myers, E.W., and Lipman, D.J. (1990). Basic local alignment search tool. *J. Mol. Biol.* 215, 403–410.
- Amaral, F.A., Sachs, D., Costa, V.V., Fagundes, C.T., Cisalpino, D., Cunha, T.M., Ferreira, S.H., Cunha, F.Q., Silva, T.A., Nicoli, J.R., et al. (2008). Commensal microbiota is fundamental for the development of inflammatory pain. *Proc. Natl. Acad. Sci. USA* 105, 2193–2197.
- Anderson, M.J., Ellingsen, K.E., and McArdle, B.H. (2006). Multivariate dispersion as a measure of beta diversity. *Ecol. Lett.* 9, 683–693.
- Atladóttir, H.O., Pedersen, M.G., Thorsen, P., Mortensen, P.B., Deleuran, B., Eaton, W.W., and Parner, E.T. (2009). Association of family history of autoimmune diseases and autism spectrum disorders. *Pediatrics* 124, 687–694.
- Atladóttir, H.O., Thorsen, P., Østergaard, L., Schendel, D.E., Lemcke, S., Abdallah, M., and Parner, E.T. (2010). Maternal infection requiring hospitalization during pregnancy and autism spectrum disorders. *J. Autism Dev. Disord.* 40, 1423–1430.
- Autism and Developmental Disabilities Monitoring Network Surveillance Year 2008 Principal Investigators; Centers for Disease Control and Prevention (2012). Prevalence of autism spectrum disorders—Autism and Developmental Disabilities Monitoring Network, 14 sites, United States, 2008. *MMWR Surveill. Summ.* 61, 1–19.
- Bauman, M.D., Iosif, A.M., Smith, S.E., Bregere, C., Amaral, D.G., and Patterson, P.H. (2013). Activation of the Maternal Immune System During Pregnancy

- Alters Behavioral Development of Rhesus Monkey Offspring. *Biol. Psychiatry*. Published online September 5, 2013. <http://dx.doi.org/10.1016/j.biopsych.2013.06.025>.
- Bercik, P., Park, A.J., Sinclair, D., Khoshdel, A., Lu, J., Huang, X., Deng, Y., Blennerhassett, P.A., Fahnstock, M., Moine, D., et al. (2011). The anxiolytic effect of *Bifidobacterium longum* NCC3001 involves vagal pathways for gut-brain communication. *Neurogastroenterol. Motil.* **23**, 1132–1139.
- Blumberg, R., and Powrie, F. (2012). Microbiota, disease, and back to health: a metastable journey. *Sci. Transl. Med.* **4**, 137rv137.
- Boukthir, S., Matoussi, N., Belhadj, A., Mammou, S., Dlala, S.B., Helayem, M., Rocchiccioli, F., Bouzaidi, S., and Abdennebi, M. (2010). [Abnormal intestinal permeability in children with autism]. *Tunis. Med.* **88**, 685–686.
- Bourin, M., Petit-Demoulière, B., Dhonnchadha, B.N., and Hascöet, M. (2007). Animal models of anxiety in mice. *Fundam. Clin. Pharmacol.* **21**, 567–574.
- Bravo, J.A., Forsythe, P., Chew, M.V., Escaravage, E., Savignac, H.M., Dinan, T.G., Bienenstock, J., and Cryan, J.F. (2011). Ingestion of *Lactobacillus* strain regulates emotional behavior and central GABA receptor expression in a mouse via the vagus nerve. *Proc. Natl. Acad. Sci. USA* **108**, 16050–16055.
- Brown, A.S., Sourander, A., Hinkka-Yli-Salomäki, S., McKeague, I.W., Sundvall, J., and Surcel, H.M. (2013). Elevated maternal C-reactive protein and autism in a national birth cohort. *Mol. Psychiatry*. Published online January 22, 2013. <http://dx.doi.org/10.1038/mp.2012.197>.
- Buie, T., Campbell, D.B., Fuchs, G.J., 3rd, Furuta, G.T., Levy, J., Vandewater, J., Whitaker, A.H., Atkins, D., Bauman, M.L., Beaudet, A.L., et al. (2010). Evaluation, diagnosis, and treatment of gastrointestinal disorders in individuals with ASDs: a consensus report. *Pediatrics* **125** (Suppl 1), S1–S18.
- Bull, G., Shattock, P., Whiteley, P., Anderson, R., Groundwater, P.W., Lough, J.W., and Lees, G. (2003). Indolyl-3-acryloylglycine (IAG) is a putative diagnostic urinary marker for autism spectrum disorders. *Med. Sci. Monit.* **9**, CR422–CR425.
- Campanozzi, A., Capano, G., Miele, E., Romano, A., Scuccimarra, G., Del Giudice, E., Strisciuglio, C., Militeri, R., and Staiano, A. (2007). Impact of malnutrition on gastrointestinal disorders and gross motor abilities in children with cerebral palsy. *Brain Dev.* **29**, 25–29.
- Collins, S.M., Surette, M., and Bercik, P. (2012). The interplay between the intestinal microbiota and the brain. *Nat. Rev. Microbiol.* **10**, 735–742.
- Comi, A.M., Zimmerman, A.W., Frye, V.H., Law, P.A., and Peeden, J.N. (1999). Familial clustering of autoimmune disorders and evaluation of medical risk factors in autism. *J. Child Neurol.* **14**, 388–394.
- Coury, D.L., Ashwood, P., Fasano, A., Fuchs, G., Geraghty, M., Kaul, A., Mawe, G., Patterson, P., and Jones, N.E. (2012). Gastrointestinal conditions in children with autism spectrum disorder: developing a research agenda. *Pediatrics* **130** (Suppl 2), S160–S168.
- Croen, L.A., Braunschweig, D., Haapanen, L., Yoshida, C.K., Fireman, B., Grether, J.K., Kharrazi, M., Hansen, R.L., Ashwood, P., and Van de Water, J. (2008). Maternal mid-pregnancy autoantibodies to fetal brain protein: the early markers for autism study. *Biol. Psychiatry* **64**, 583–588.
- Cryan, J.F., and Dinan, T.G. (2012). Mind-altering microorganisms: the impact of the gut microbiota on brain and behaviour. *Nat. Rev. Neurosci.* **13**, 701–712.
- D'Eufemia, P., Celli, M., Finocchiaro, R., Pacifico, L., Viozzi, L., Zaccagnini, M., Cardi, E., and Giardini, O. (1996). Abnormal intestinal permeability in children with autism. *Acta Paediatr.* **85**, 1076–1079.
- de Magistris, L., Familiari, V., Pascotto, A., Sapone, A., Frolli, A., Iardino, P., Carteni, M., De Rosa, M., Francavilla, R., Riegler, G., et al. (2010). Alterations of the intestinal barrier in patients with autism spectrum disorders and in their first-degree relatives. *J. Pediatr. Gastroenterol. Nutr.* **51**, 418–424.
- Desbonnet, L., Clarke, G., Shanahan, F., Dinan, T.G., and Cryan, J.F. (2013). Microbiota is essential for social development in the mouse. *Mol. Psychiatry*. Published online May 21, 2013. <http://dx.doi.org/10.1038/mp.2013.65>.
- Diaz Heijtz, R., Wang, S., Anuar, F., Qian, Y., Björkholm, B., Samuelsson, A., Hibberd, M.L., Forssberg, H., and Pettersson, S. (2011). Normal gut microbiota modulates brain development and behavior. *Proc. Natl. Acad. Sci. USA* **108**, 3047–3052.
- Fierer, N., Lauber, C.L., Zhou, N., McDonald, D., Costello, E.K., and Knight, R. (2010). Forensic identification using skin bacterial communities. *Proc. Natl. Acad. Sci. USA* **107**, 6477–6481.
- Finegold, S.M., Dowd, S.E., Gontcharova, V., Liu, C., Henley, K.E., Wolcott, R.D., Youn, E., Summanen, P.H., Granpeesheh, D., Dixon, D., et al. (2010). Pyrosequencing study of fecal microflora of autistic and control children. *Anaerobe* **16**, 444–453.
- Finegold, S.M., Downes, J., and Summanen, P.H. (2012). Microbiology of regressive autism. *Anaerobe* **18**, 260–262.
- Gondalia, S.V., Palombo, E.A., Knowles, S.R., Cox, S.B., Meyer, D., and Austin, D.W. (2012). Molecular characterisation of gastrointestinal microbiota of children with autism (with and without gastrointestinal dysfunction) and their neurotypical siblings. *Autism Res.* **5**, 419–427.
- Gorringo, P., Williams, K.C., Lee, E.B., Walker, L.S., McGrew, S.G., and Levitt, P. (2012). Gastrointestinal dysfunction in autism: parental report, clinical evaluation, and associated factors. *Autism Res.* **5**, 101–108.
- Graff, L.A., Walker, J.R., and Bernstein, C.N. (2009). Depression and anxiety in inflammatory bowel disease: a review of comorbidity and management. *Inflamm. Bowel Dis.* **15**, 1105–1118.
- Grimsley, J.M., Monaghan, J.J., and Wenstrup, J.J. (2011). Development of social vocalizations in mice. *PLoS ONE* **6**, e17460.
- Hallmayer, J., Cleveland, S., Torres, A., Phillips, J., Cohen, B., Torigoe, T., Miller, J., Fedele, A., Collins, J., Smith, K., et al. (2011). Genetic heritability and shared environmental factors among twin pairs with autism. *Arch. Gen. Psychiatry* **68**, 1095–1102.
- Ibrahim, S.H., Voigt, R.G., Katusic, S.K., Weaver, A.L., and Barbaresi, W.J. (2009). Incidence of gastrointestinal symptoms in children with autism: a population-based study. *Pediatrics* **124**, 680–686.
- Kang, D.W., Park, J.G., Ilhan, Z.E., Wallstrom, G., Labaer, J., Adams, J.B., and Krajmalnik-Brown, R. (2013). Reduced incidence of *Prevotella* and other fermenters in intestinal microflora of autistic children. *PLoS ONE* **8**, e68322.
- Keszthelyi, D., Troost, F.J., and Masclee, A.A. (2009). Understanding the role of tryptophan and serotonin metabolism in gastrointestinal function. *Neurogastroenterol. Motil.* **21**, 1239–1249.
- Kohane, I.S., McMurry, A., Weber, G., MacFadden, D., Rappaport, L., Kunkel, L., Bickel, J., Wattanasin, N., Spence, S., Murphy, S., and Churchill, S. (2012). The co-morbidity burden of children and young adults with autism spectrum disorders. *PLoS ONE* **7**, e33224.
- Lafaye, A., Junot, C., Ramounet-Le Gall, B., Fritsch, P., Ezan, E., and Tabet, J.C. (2004). Profiling of sulfoconjugates in urine by using precursor ion and neutral loss scans in tandem mass spectrometry. Application to the investigation of heavy metal toxicity in rats. *J. Mass Spectrom.* **39**, 655–664.
- Li, Q., Cheung, C., Wei, R., Hui, E.S., Feldon, J., Meyer, U., Chung, S., Chua, S.E., Sham, P.C., Wu, E.X., and McAlonan, G.M. (2009). Prenatal immune challenge is an environmental risk factor for brain and behavior change relevant to schizophrenia: evidence from MRI in a mouse model. *PLoS ONE* **4**, e6354.
- Malkova, N.V., Yu, C.Z., Hsiao, E.Y., Moore, M.J., and Patterson, P.H. (2012). Maternal immune activation yields offspring displaying mouse versions of the three core symptoms of autism. *Brain Behav. Immun.* **26**, 607–616.
- Mazmanian, S.K., Round, J.L., and Kasper, D.L. (2008). A microbial symbiosis factor prevents intestinal inflammatory disease. *Nature* **453**, 620–625.
- Messaoudi, M., Lalonde, R., Violle, N., Javelot, H., Desor, D., Nejd, A., Bisson, J.F., Rougeot, C., Pichelin, M., Cazaubiel, M., and Cazaubiel, J.M. (2011). Assessment of psychotropic-like properties of a probiotic formulation (*Lactobacillus helveticus* R0052 and *Bifidobacterium longum* R0175) in rats and human subjects. *Br. J. Nutr.* **105**, 755–764.
- Motil, K.J., Caeg, E., Barrish, J.O., Geerts, S., Lane, J.B., Percy, A.K., Anness, F., McNair, L., Skinner, S.A., Lee, H.S., et al. (2012). Gastrointestinal and nutritional problems occur frequently throughout life in girls and women with Rett syndrome. *J. Pediatr. Gastroenterol. Nutr.* **55**, 292–298.
- Nicholson, J.K., Holmes, E., Kinross, J., Burcelin, R., Gibson, G., Jia, W., and Pettersson, S. (2012). Host-gut microbiota metabolic interactions. *Science* **336**, 1262–1267.

- Ochoa-Repáraz, J., Mielcarz, D.W., Ditrío, L.E., Burroughs, A.R., Begum-Haque, S., Dasgupta, S., Kasper, D.L., and Kasper, L.H. (2010). Central nervous system demyelinating disease protection by the human commensal *Bacteroides fragilis* depends on polysaccharide A expression. *J. Immunol.* *185*, 4101–4108.
- Onore, C., Careaga, M., and Ashwood, P. (2012). The role of immune dysfunction in the pathophysiology of autism. *Brain Behav. Immun.* *26*, 383–392.
- Parracho, H.M., Bingham, M.O., Gibson, G.R., and McCartney, A.L. (2005). Differences between the gut microflora of children with autistic spectrum disorders and that of healthy children. *J. Med. Microbiol.* *54*, 987–991.
- Peñagarikano, O., Abrahams, B.S., Herman, E.I., Winden, K.D., Gdalyahu, A., Dong, H., Sonnenblick, L.I., Gruver, R., Almajano, J., Bragin, A., et al. (2011). Absence of CNTNAP2 leads to epilepsy, neuronal migration abnormalities, and core autism-related deficits. *Cell* *147*, 235–246.
- Perry, W., Minassian, A., Lopez, B., Maron, L., and Lincoln, A. (2007). Sensorimotor gating deficits in adults with autism. *Biol. Psychiatry* *61*, 482–486.
- Persico, A.M., and Napolioni, V. (2013). Urinary p-cresol in autism spectrum disorder. *Neurotoxicol. Teratol.* *36*, 82–90.
- Rao, A.V., Bested, A.C., Beaulne, T.M., Katzman, M.A., Iorio, C., Berardi, J.M., and Logan, A.C. (2009). A randomized, double-blind, placebo-controlled pilot study of a probiotic in emotional symptoms of chronic fatigue syndrome. *Gut Pathog* *1*, 6.
- Robertson, M.A., Sigalet, D.L., Holst, J.J., Meddings, J.B., Wood, J., and Sharkey, K.A. (2008). Intestinal permeability and glucagon-like peptide-2 in children with autism: a controlled pilot study. *J. Autism Dev. Disord.* *38*, 1066–1071.
- Round, J.L., and Mazmanian, S.K. (2010). Inducible Foxp3+ regulatory T-cell development by a commensal bacterium of the intestinal microbiota. *Proc. Natl. Acad. Sci. USA* *107*, 12204–12209.
- Shi, L., Smith, S.E., Malkova, N., Tse, D., Su, Y., and Patterson, P.H. (2009). Activation of the maternal immune system alters cerebellar development in the offspring. *Brain Behav. Immun.* *23*, 116–123.
- Silverman, J.L., Yang, M., Lord, C., and Crawley, J.N. (2010). Behavioural phenotyping assays for mouse models of autism. *Nat. Rev. Neurosci.* *11*, 490–502.
- Smith, E.A., and Macfarlane, G.T. (1997). Formation of Phenolic and Indolic Compounds by Anaerobic Bacteria in the Human Large Intestine. *Microb. Ecol.* *33*, 180–188.
- Smith, S.E., Li, J., Garbett, K., Mirnics, K., and Patterson, P.H. (2007). Maternal immune activation alters fetal brain development through interleukin-6. *J. Neurosci.* *27*, 10695–10702.
- Thomas, A., Burant, A., Bui, N., Graham, D., Yuva-Paylor, L.A., and Paylor, R. (2009). Marble burying reflects a repetitive and perseverative behavior more than novelty-induced anxiety. *Psychopharmacology (Berl.)* *204*, 361–373.
- Tillisch, K., Labus, J., Kilpatrick, L., Jiang, Z., Stains, J., Ebrat, B., Guyonnet, D., Legrain-Raspaud, S., Trotin, B., Naliboff, B., and Mayer, E.A. (2013). Consumption of fermented milk product with probiotic modulates brain activity. *Gastroenterology* *144*, 1394–1401, e1–e4.
- Turner, J.R. (2009). Intestinal mucosal barrier function in health and disease. *Nat. Rev. Immunol.* *9*, 799–809.
- Wikoff, W.R., Anfora, A.T., Liu, J., Schultz, P.G., Lesley, S.A., Peters, E.C., and Siuzdak, G. (2009). Metabolomics analysis reveals large effects of gut microflora on mammalian blood metabolites. *Proc. Natl. Acad. Sci. USA* *106*, 3698–3703.
- Williams, B.L., Hornig, M., Buie, T., Bauman, M.L., Cho Paik, M., Wick, I., Bennett, A., Jabado, O., Hirschberg, D.L., and Lipkin, W.I. (2011). Impaired carbohydrate digestion and transport and mucosal dysbiosis in the intestines of children with autism and gastrointestinal disturbances. *PLoS ONE* *6*, e24585.
- Williams, B.L., Hornig, M., Parekh, T., and Lipkin, W.I. (2012). Application of novel PCR-based methods for detection, quantitation, and phylogenetic characterization of *Sutterella* species in intestinal biopsy samples from children with autism and gastrointestinal disturbances. *MBio* *3*, e00261–e11.

EXTENDED EXPERIMENTAL PROCEDURES

B. fragilis Treatment

At 3 weeks of age, saline and poly(I:C) offspring across individual litters were weaned into cages of 4 nonlittermate offspring of the same treatment group to generate a randomized experimental design (Lazic, 2013). Cages within the poly(I:C) versus saline treatment groups were selected at random for treatment with nonenterotoxigenic *B. fragilis* NCTC 9343 (Sears, 2009) or vehicle, every other day for 6 days. To preclude any confounding effects of early life stress on neurodevelopment and behavior, suspensions were not administered by oral gavage. For *B. fragilis* treatment, 10^{10} cfu freshly grown *B. fragilis* was suspended in 1 ml 1.5% sodium bicarbonate, mixed with 4 ml sugar-free applesauce and spread over four standard food pellets. We find that ~42% of *B. fragilis* colony forming units are recovered from the applesauce inoculum at 48 hr after administration, suggesting that both viable and nonviable *B. fragilis* is ingested during the treatment. For vehicle treatment, saline and poly(I:C) animals were fed 1.5% sodium bicarbonate in applesauce over food pellets. Applesauce and pellets were completely consumed by mice of each treatment group by 48 hr after administration. The same procedure was used for treatment with mutant *B. fragilis* lacking PSA and *B. thetaiotaomicron*.

Intestinal qRT-PCR, Western Blots, and Cytokine Profiles

Gut tissue was flushed with HBSS and either (1) homogenized in Trizol for RNA isolation and reverse transcription according to Hsiao and Patterson (2011) or (2) homogenized in Tissue Extraction Reagent I (Invitrogen) containing protease inhibitors (Roche) for protein assays. For cytokine profiling, mouse 20-plex cytokine arrays (Invitrogen) were run on the Luminex FLEXMAP 3D platform by the Clinical Immunobiology Correlative Studies Laboratory at the City of Hope (Duarte, CA). Western blots were conducted according to standard methods and probed with rabbit anti-claudin 8 or rabbit anti-claudin 15 (Invitrogen) at 1:100 dilution.

Microbial DNA Extraction, 16S rRNA Gene Amplification and Pyrosequencing

For each experimental group, 10 mice (5 males, 5 females) from different litters were randomly selected for single housing at weaning and treatment with either vehicle or *B. fragilis*, as described above. Bacterial genomic DNA was extracted from mouse fecal pellets using the MoBio PowerSoil Kit following protocols benchmarked as part of the NIH Human Microbiome Project. The V3-V5 regions of the 16S rRNA gene were PCR amplified using individually barcoded universal primers containing linker sequences for 454-pyrosequencing. Sequencing was performed at the HGSC at BCM using a multiplexed 454-Titanium pyrosequencer.

16S rRNA Gene Sequence Analysis

FASTA and quality files were obtained from the Alkek Center for Metagenomics and Microbiome Research at the Baylor College of Medicine. 16S data were processed and its diversity was analyzed using QIIME 1.6 software package (Caporaso et al., 2010b) as follows. Sequences < 200 bp and > 1,000 bp, and sequences containing any primer mismatches, barcode mismatches, ambiguous bases, homopolymer runs exceeding six bases, or an average quality score of below 30 were discarded and the remaining sequences were checked for chimeras and clustered to operational taxonomic units (OTUs) using the USearch pipeline (Edgar, 2010; Edgar et al., 2011) with a sequence similarity index of 97%. OTUs were subsequently assigned taxonomic classification using the basic local alignment search tool (BLAST) classifier (Altschul et al., 1990), based on the small subunit nonredundant reference database release 111 (Quast et al., 2013) with 0.001 maximum e-value. These taxonomies were then used to generate taxonomic summaries of all OTUs at different taxonomic levels. For tree-based alpha- and beta diversity analyses, representative sequences for each OTU were aligned using PyNAST (Caporaso et al., 2010a) and a phylogenetic tree was constructed based on this alignment using FastTree (Price et al., 2009). Alpha diversity estimates (by Observed Species and Faith's phylogenetic diversity [PD]; Faith, 1992) and evenness (by Simpson's evenness and Gini Coefficient; Wittebolle et al., 2009) were calculated and compared between groups using a nonparametric test based on 100 iterations using a rarefaction of 2,082 sequences from each sample. For beta diversity, even sampling of 2,160 sequences per sample was used, and calculated using weighted and unweighted UniFrac (Lozupone and Knight, 2005). Beta diversity was compared in a pairwise fashion (S versus P, P versus P+BF), from unweighted UniFrac distance matrixes, using the analysis of similarity (ANOSIM; Fierer et al., 2010), permutational multivariate analysis of variance (PERMANOVA; Anderson, 2008; McArdle and Anderson, 2001), permutational analysis of multivariate dispersions (PERMDISP; Anderson et al., 2006), and Moran's I, each with 999 permutations to determine statistical significance.

Identification of Differences in Specific OTUs

Key OTUs, that discriminate between Saline and Poly(I:C) treatment groups, and between Poly(I:C) and Poly(I:C) + *B. fragilis* treatment groups, were identified using an unbiased method from OTU tables, generated by QIIME, using three complimentary analyses: (1) Metastats comparison (White et al., 2009) and (2) the Random Forests algorithm, first under QIIME (Knights et al., 2011) and subsequently coupled with Boruta feature selection, in the GenBoree microbiome toolset (Riehle et al., 2012), and (3) the Galaxy platform-based LDA Effect Size analysis (LEfSe; Segata et al., 2011). Only OTUs that differ significantly between treatment groups were candidates for further analyses ($p < 0.05$ for [1] and [3], and > 0.0001 mean decrease in accuracy for Random Forests and subsequent identification by the Boruta algorithm). Metastats analyses were done using the online interface (<http://metastats.cbcb.umd.edu>) with QIIME-generated OTU tables of any two treatment groups. The Random Forests algorithm was used to identify discriminatory OTUs in the QIIME software package (Breiman, 2001; Knights et al., 2011), comparing two treatment groups at a time,

based on 1,000 trees and a 10-fold cross-validation, and was further validated and coupled with the Boruta feature selection algorithm, as implemented in the Genboree Microbiome toolset (Kursa and Rudnicki, 2010; Riehle et al., 2012). Only those OTUs that were confirmed by the Boruta algorithm were defined as discriminatory. The ratio between observed and calculated error rates was used as a measure of confidence for Random Forests Analyses: this ratio was 5.0 for saline versus poly(I:C) (with an estimated error of 0.1 ± 0.21) and 2.86 for poly(I:C) versus poly(I:C) + *B. fragilis* (with an estimated error of 0.23 ± 0.22). In order to overcome any misidentification by any one of the three methods only OTUs that were identified by at least two of the three above methods were defined as discriminatory. For the analyses in Figure 1 and Table S1, OTUs that were significantly altered by MIA were identified by comparing the saline versus poly(I:C) groups. For the analyses in Figure 3, we compared the poly(I:C) versus poly(I:C)+*B. fragilis* groups, and only report only those OTUs that have also been identified by the analyses in Figure 1 and Table S1. In addition, we compared the results obtained by Random Forests Analysis with feature selection by Boruta to those obtained by Random Forests Analysis with a cutoff of 0.001 mean decrease in accuracy.

To generate a phylogenetic tree depicting the closest cultured type strains to key OTUs identified, key OTUs were then aligned using the SINA aligner (<http://www.arb-silva.de/aligner/>; (Pruesse et al., 2012), compared to the SILVA reference database release 111 (Quast et al., 2013) using Arb (Ludwig et al., 2004) and visualized using FigTree (<http://tree.bio.ed.ac.uk/software/figtree/>). Heat maps of key OTUs were generated by extracting their relative abundance from the OTU table. These data were then normalized (so that the sum of squares of all values in a row or column equals one), first by OTU and subsequently by sample, and clustered by correlation using Cluster 3.0 (de Hoon et al., 2004). Finally, abundance data were visualized using Java TreeView (Saldanha, 2004).

Metabolomics Screening

Sera were collected by cardiac puncture from behaviorally validated adult mice. Samples were extracted and analyzed on GC/MS, LC/MS and LC/MS/MS platforms by Metabolon, Inc. Protein fractions were removed by serial extractions with organic aqueous solvents, concentrated using a TurboVap system (Zymark) and vacuum dried. For LC/MS and LC/MS/MS, samples were reconstituted in acidic or basic LC-compatible solvents containing > 11 injection standards and run on a Waters ACQUITY UPLC and Thermo-Finnigan LTQ mass spectrometer, with a linear ion-trap front-end and a Fourier transform ion cyclotron resonance mass spectrometer back-end. For GC/MS, samples were derivatized under dried nitrogen using bistrimethyl-silyl-trifluoroacetamide and analyzed on a Thermo-Finnigan Trace DSQ fast-scanning single-quadrupole mass spectrometer using electron impact ionization. Chemical entities were identified by comparison to metabolomic library entries of purified standards. Following log transformation and imputation with minimum observed values for each compound, data were analyzed using two-way ANOVA with contrasts.

In Vitro Immune Assays

Methods for Treg and Gr-1 flow cytometry and CD4+ T cell in vitro stimulation are described in Hsiao et al. (2012). Briefly, cells were harvested in complete RPMI from spleens and mesenteric lymph nodes. For subtyping of splenocytes, cells were stained with Gr-1 APC, CD11b-PE, CD4-FITC and Ter119-PerCP-Cy5.5 (Biolegend). For detection of Tregs, splenocytes were stimulated for 4 hr with PMA/ionomycin in the presence of GolgiPLUG (BD Biosciences), blocked for Fc receptors and labeled with CD4-FITC, CD25-PE, Foxp3-APC and Ter119-PerCP-Cy5.5. Samples were processed using the FACSCalibur cytometer (BD Biosciences) and analyzed using FlowJo software (TreeStar). For CD4+ T cell stimulation assays, 10^6 CD4+ T cells were cultured in complete RPMI with PMA (50 ng/ml) and ionomycin (750 ng/ml) for 3 d at 37C with 5% (vol/vol) CO₂. Each day, supernatant was collected for ELISA assays to detect IL-6 and IL-17, according to the manufacturer's instructions (eBioscience).

B. fragilis Colonization Assay

Fecal samples were sterilely collected from MIA and control offspring at 1, 2, and 3 weeks after the start of treatment with *B. fragilis* or vehicle. Germ-free mice were treated with *B. fragilis* as described above to serve as positive controls. DNA was isolated from fecal samples using the QIAamp DNA Stool Mini Kit (QIAGEN). 50 ng DNA was used for qPCR with *B. fragilis*-specific, 5' TGATTCCG CATGGTTTCATT 3' and 5' CGACCCATAGAGCCTTCATC 3', and universal 16S primers 5' ACTCCTACGGGAGGCAGCAGT 3' and 5' ATTACCGCGGCTGCTGGC 3' according to Odamaki et al. (2008).

Behavioral Testing

Mice were tested beginning at 6 weeks of age for PPI, open field exploration, marble burying, social interaction and adult ultrasonic vocalizations, in that order, with at least 5 days between behavioral tests. Behavioral data for *B. fragilis* treatment and control groups (Figure 5) represent cumulative results collected from multiple litters of 3-5 independent cohorts of mice for PPI and open field tests, 2-4 cohorts for marble burying, 2 cohorts for adult male ultrasonic vocalization and 1 cohort for social interaction. Discrepancies in sample size across behavioral tests reflect differences in when during our experimental study a particular test was implemented.

Prepulse Inhibition

PPI tests are used as a measure of sensorimotor gating and were conducted and analyzed as in Geyer and Swerdlow (2001) and (Smith et al., 2007). Briefly, mice were acclimated to the testing chambers of the SR-LAB startle response system (San Diego Instruments) for 5 min, presented with six 120 db pulses of white noise (startle stimulus) and then subjected to 14 randomized blocks of either no startle, startle stimulus only, 5 db prepulse with startle or 15 db prepulse with startle. The startle response was recorded by a

piezo-electric sensor, and the percent PPI is defined as: $[(\text{startle stimulus only} - 5 \text{ or } 15 \text{ db prepulse with startle})/\text{startle stimulus only}] * 100$.

Open field exploration. The open field test is widely used to measure anxiety-like and locomotor behavior in rodents. Mice were placed in 50 × 50 cm white Plexiglas boxes for 10 min. An overhead video camera recorded the session, and Ethovision software (Noldus) was used to analyze the distance traveled, and the number of entries and duration of time spent in the center arena (central 17 cm square).

Marble Burying

Marble burying is an elicited repetitive behavior in rodents analogous to those observed in autistic individuals (Silverman et al., 2010). This test was conducted and analyzed according to methods described in Thomas et al., (2009) and (Malkova et al., 2012). Mice were habituated for 10 min to a novel testing cage containing a 4 cm layer of chipped cedar wood bedding and then transferred to a new housing cage. 18 glass marbles (15 mm diameter) were aligned equidistantly 6 × 3 in the testing cage. Mice were returned to the testing cage and the number of marbles buried in 10 min was recorded.

Sociability and Social Preference

Social interaction tests were conducted and analyzed according to methods adopted from Sankoorikal et al. (2006) and (Yang et al., 2011). Briefly, testing mice were habituated for 10 min to a 50 × 75 cm Plexiglas three-chambered apparatus containing clear interaction cylinders in each of the side chambers. Sociability was tested in the following 10 min session, where the testing mouse was given the opportunity to explore a novel same-sex, age-matched mouse in one interaction cylinder (social object) versus a novel toy (green sticky ball) in the other interaction cylinder of the opposite chamber. Social preference was tested in the final 10 min session, where the testing mouse was given the opportunity to explore a now familiar mouse (stimulus mouse from the previous sociability session) versus a novel unfamiliar same-sex, age-matched mouse. In each session, the trajectory of the testing mouse was tracked with Ethovision software (Noldus). Sociability data are presented as preference for the mouse over the toy: percent of time in the social chamber - percent of time in the nonsocial chamber, and social preference data are presented as preference for the unfamiliar mouse over the familiar mouse: percent of time in the unfamiliar mouse chamber—percent of time in the familiar mouse chamber. Similar indexes were measured for chamber entries, and entries into and duration spent in the contact zone (7 × 7 cm square surrounding the interaction cylinder).

Adult Ultrasonic Vocalizations

Male mice produce USVs in response to female mice as an important form of communication (Portfors, 2007). We measured adult male USV production in response to novel female exposure according to methods described in Grimsley et al. (2011), Scattoni et al. (2011), and Silverman et al. (2010). Adult males were single-housed one week before testing and exposed for 20 min to an unfamiliar adult female mouse each day starting four days prior to testing in order to provide a standardized history of sexual experience and to adjust for differences in social dominance. On testing day, mice were habituated to a novel cage for 10 min before exposure to a novel age-matched female. USVs were recorded for 3 min using the UltraSoundGate microphone and audio system (Avisoft Bioacoustics). Recordings were analyzed using Avisoft's SASLab Pro software after fast Fourier transformation at 512 FFT-length and detection by a threshold-based algorithm with 5 ms hold time. Data presented reflect duration and number of calls produced in the 3 min session.

4EPS Synthesis and Detection

Potassium 4-ethylphenylsulfate was prepared using a modification of a procedure reported for the synthesis of aryl sulfates in Burlingham et al. (2003) and Grimes (1959) (Figure S7A). 4-ethylphenol (Sigma-Aldrich, 5.00 g, 40.9 mmol) was treated with sulfur trioxide-pyridine complex (Sigma-Aldrich, 5.92 g, 37.2 mmol) in refluxing benzene (20 ml, dried by passing through an activated alumina column). After 3.5 hr, the resulting solution was cooled to room temperature, at which point the product crystallized. Isolation by filtration afforded 7.93 g of crude pyridinium 4-ethylphenylsulfate as a white crystalline solid. 1.00 g of this material was dissolved in 10 ml of 3% triethylamine in acetonitrile and filtered through a plug of silica gel (Silicycle, particle size 32–63 μm), eluting with 3% triethylamine in acetonitrile. The filtrate was then concentrated, and the resulting residue was dissolved in 20 ml of deionized water and eluted through a column of Dowex 50WX8 ion exchange resin (K⁺ form), rinsing with 20 ml of deionized water. The ion exchange process was repeated once more, and the resulting solution concentrated under vacuum to afford 618 mg (55% overall yield) of potassium 4-ethylphenylsulfate as a white powder (Figure S7A).

¹H and ¹³C NMR spectra of authentic potassium 4-ethylphenylsulfate were recorded on a Varian Inova 500 spectrometer and are reported relative to internal DMSO-*d*₅ (¹H, δ = 2.50; ¹³C, δ = 39.52). A high-resolution mass spectrum (HRMS) was acquired using an Agilent 6200 Series TOF with an Agilent G1978A Multimode source in mixed ionization mode (electrospray ionization [ESI] and atmospheric pressure chemical ionization [APCI]). Spectroscopic data for potassium 4-ethylphenylsulfate are as follows: ¹H NMR (DMSO-*d*₆, 500 MHz) δ 7.11 – 7.04 (m, 4H), 2.54 (q, *J* = 7.6 Hz, 2H), 1.15 (t, *J* = 7.6 Hz, 3H); ¹³C NMR (DMSO-*d*₆, 126 MHz) δ 151.4, 138.3, 127.9, 120.6, 27.5, 16.0; HRMS (Multimode-ESI/APCI) calculated for C₈H₉O₄S [M–K]⁺ 201.0227, found 201.0225.

Authentic 4EPS and serum samples were analyzed by LC/MS using an Agilent 110 Series HPLC system equipped with a photodiode array detector and interfaced to a model G1946C single-quadrupole electrospray mass spectrometer. HPLC separations were obtained at 25°C using an Agilent Zorbax XDB-C18 column (4.6 mm × 50 mm × 5 μm particle size). The 4EPS ion was detected using selected ion monitoring for ions of *m/z* 200.9 and dwell time of 580 ms/ion, with the electrospray capillary set at 3 kV. Authentic potassium 4EPS was found to possess a retention time of 6.2 min when eluted in 0.05% trifluoroacetic acid and acetonitrile, using a 10 min linear gradient from 0%–50% acetonitrile. For quantification of 4EPS in mouse sera, a dose-response curve was constructed

by plotting the total ion count peak area for known concentrations of authentic potassium 4EPS against the analyte concentration ($R^2 = 0.9998$; [Figure S7B](#)). Mouse serum samples were diluted 4-fold with acetonitrile and centrifuged at 10,000 g at 4°C for 3 min. 10 μ l of supernatant was injected directly into the HPLC system.

SUPPLEMENTAL REFERENCES

- Anderson, M.J. (2008). A new method for non-parametric multivariate analysis of variance. *Austral Ecol.* *26*, 32–46.
- Breiman, L. (2001). Random forests. *Mach. Learn.* *45*, 5–32.
- Burlingham, B.T., Pratt, L.M., Davidson, E.R., Shiner, V.J., Jr., Fong, J., and Widlanski, T.S. (2003). ^{34}S isotope effect on sulfate ester hydrolysis: mechanistic implications. *J. Am. Chem. Soc.* *125*, 13036–13037.
- Caporaso, J.G., Bittinger, K., Bushman, F.D., DeSantis, T.Z., Andersen, G.L., and Knight, R. (2010a). PyNAST: a flexible tool for aligning sequences to a template alignment. *Bioinformatics* *26*, 266–267.
- Caporaso, J.G., Kuczynski, J., Stombaugh, J., Bittinger, K., Bushman, F.D., Costello, E.K., Fierer, N., Peña, A.G., Goodrich, J.K., Gordon, J.I., et al. (2010b). QIIME allows analysis of high-throughput community sequencing data. *Nat. Methods* *7*, 335–336.
- de Hoon, M.J.L., Imoto, S., Nolan, J., and Miyano, S. (2004). Open source clustering software. *Bioinformatics* *20*, 1453–1454.
- Edgar, R.C. (2010). Search and clustering orders of magnitude faster than BLAST. *Bioinformatics* *26*, 2460–2461.
- Edgar, R.C., Haas, B.J., Clemente, J.C., Quince, C., and Knight, R. (2011). UCHIME improves sensitivity and speed of chimera detection. *Bioinformatics* *27*, 2194–2200.
- Faith, D.P. (1992). Conservation Evaluation and Phylogenetic Diversity. *Biol. Conserv.* *61*, 1–10.
- Geyer, M.A., and Swerdlow, N.R. (2001). Measurement of startle response, prepulse inhibition, and habituation. *Curr Protoc Neurosci Chapter 8*, Unit 8 7.
- Grimes, A.J. (1959). Synthesis of ^{35}S -labelled arylsulphates by intact animals and by tissue preparations, with particular reference to L-tyrosine O-sulphate. *Biochem. J.* *73*, 723–729.
- Hsiao, E.Y., McBride, S.W., Chow, J., Mazmanian, S.K., and Patterson, P.H. (2012). Modeling an autism risk factor in mice leads to permanent immune dysregulation. *Proc. Natl. Acad. Sci. USA* *109*, 12776–12781.
- Hsiao, E.Y., and Patterson, P.H. (2011). Activation of the maternal immune system induces endocrine changes in the placenta via IL-6. *Brain Behav. Immun.* *25*, 604–615.
- Knights, D., Costello, E.K., and Knight, R. (2011). Supervised classification of human microbiota. *FEMS Microbiol. Rev.* *35*, 343–359.
- Kursa, M.B., and Rudnicki, W.R. (2010). Feature Selection with the Boruta Package. *J. Stat. Softw.* *36*, 1–13.
- Lazic, S.E. (2013). Comment on “Stress in puberty unmasks latent neuropathological consequences of prenatal immune activation in mice”. *Science* *340*, 811.
- Lozupone, C., and Knight, R. (2005). UniFrac: a new phylogenetic method for comparing microbial communities. *Appl. Environ. Microbiol.* *71*, 8228–8235.
- Ludwig, W., Strunk, O., Westram, R., Richter, L., Meier, H., Yadhukumar, Buchner, A., Lai, T., Steppi, S., Jobb, G., et al. (2004). ARB: a software environment for sequence data. *Nucleic Acids Res.* *32*, 1363–1371.
- McArdle, B.H., and Anderson, M.J. (2001). Fitting multivariate models to community data: a comment on distancebased redundancy analysis. *Ecology* *82*, 290–297.
- Odamaki, T., Xiao, J.Z., Sakamoto, M., Kondo, S., Yaeshima, T., Iwatsuki, K., Togashi, H., Enomoto, T., and Benno, Y. (2008). Distribution of different species of the *Bacteroides fragilis* group in individuals with Japanese cedar pollinosis. *Appl. Environ. Microbiol.* *74*, 6814–6817.
- Portfors, C.V. (2007). Types and functions of ultrasonic vocalizations in laboratory rats and mice. *J. Am. Assoc. Lab. Anim. Sci.* *46*, 28–34.
- Price, M.N., Dehal, P.S., and Arkin, A.P. (2009). FastTree: computing large minimum evolution trees with profiles instead of a distance matrix. *Mol. Biol. Evol.* *26*, 1641–1650.
- Pruesse, E., Peplies, J., and Glöckner, F.O. (2012). SINA: accurate high-throughput multiple sequence alignment of ribosomal RNA genes. *Bioinformatics* *28*, 1823–1829.
- Quast, C., Pruesse, E., Yilmaz, P., Gerken, J., Schweer, T., Yarza, P., Peplies, J., and Glöckner, F.O. (2013). The SILVA ribosomal RNA gene database project: improved data processing and web-based tools. *Nucleic Acids Res.* *41* (Database issue), D590–D596.
- Riehle, K., Coarfa, C., Jackson, A., Ma, J., Tandon, A., Paithankar, S., Raghuraman, S., Mistretta, T.A., Saulnier, D., Raza, S., et al. (2012). The Genboree Microbiome Toolset and the analysis of 16S rRNA microbial sequences. *BMC Bioinformatics* *13* (Suppl 13), S11.
- Saldanha, A.J. (2004). Java Treeview—extensible visualization of microarray data. *Bioinformatics* *20*, 3246–3248.
- Sankoorikal, G.M., Kaercher, K.A., Boon, C.J., Lee, J.K., and Brodtkin, E.S. (2006). A mouse model system for genetic analysis of sociability: C57BL/6J versus BALB/cJ inbred mouse strains. *Biol. Psychiatry* *59*, 415–423.
- Scattoni, M.L., Ricceri, L., and Crawley, J.N. (2011). Unusual repertoire of vocalizations in adult BTBR T+tf/J mice during three types of social encounters. *Genes Brain Behav.* *10*, 44–56.
- Sears, C.L. (2009). Enterotoxigenic *Bacteroides fragilis*: a rogue among symbiotes. *Clin. Microbiol. Rev.* *22*, 349–369.
- Segata, N., Izard, J., Waldron, L., Gevers, D., Miropolsky, L., Garrett, W.S., and Huttenhower, C. (2011). Metagenomic biomarker discovery and explanation. *Genome Biol.* *12*, R60.
- White, J.R., Nagarajan, N., and Pop, M. (2009). Statistical methods for detecting differentially abundant features in clinical metagenomic samples. *PLoS Comput. Biol.* *5*, e1000352.
- Wittebolle, L., Marzorati, M., Clement, L., Balloi, A., Daffonchio, D., Heylen, K., De Vos, P., Verstraete, W., and Boon, N. (2009). Initial community evenness favours functionality under selective stress. *Nature* *458*, 623–626.
- Yang, M., Silverman, J.L., and Crawley, J.N. (2011). Automated three-chambered social approach task for mice. *Curr Protoc Neurosci Chapter 8*, Unit 8 26.

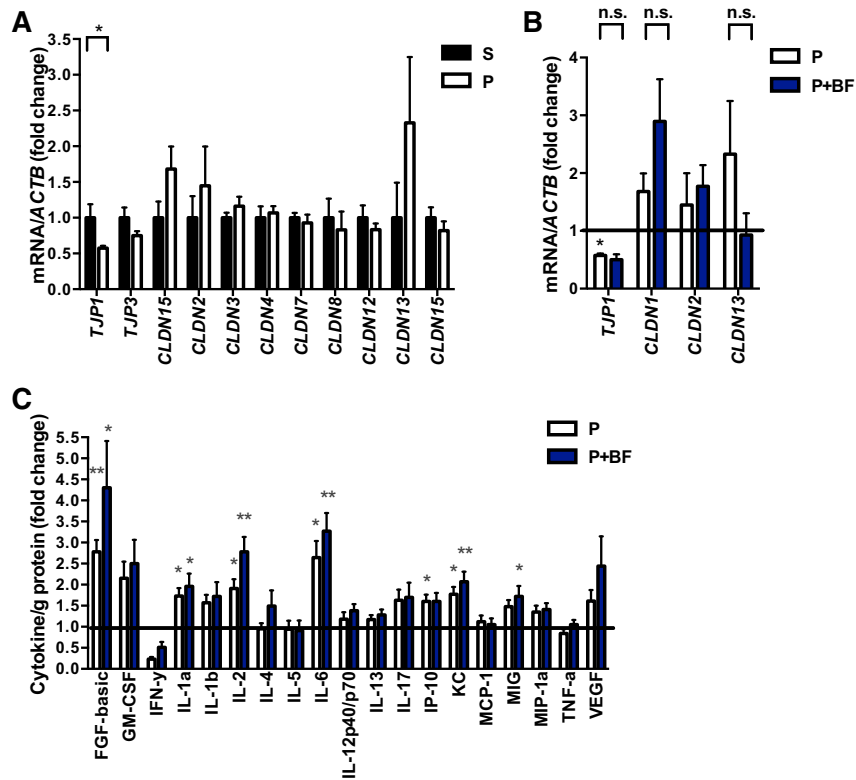


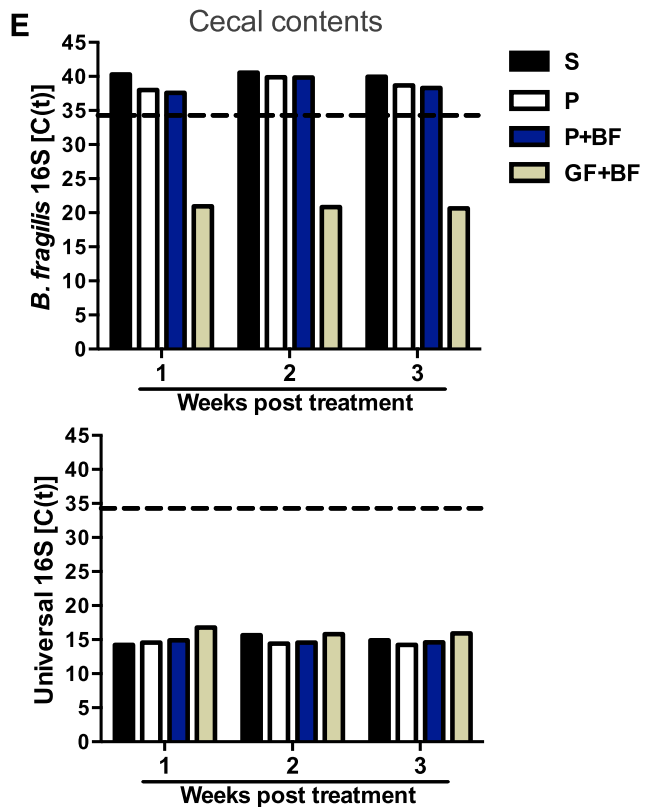
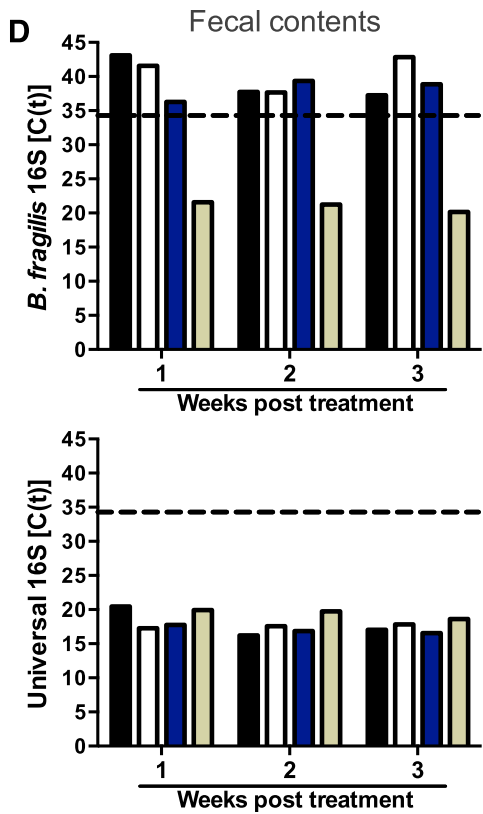
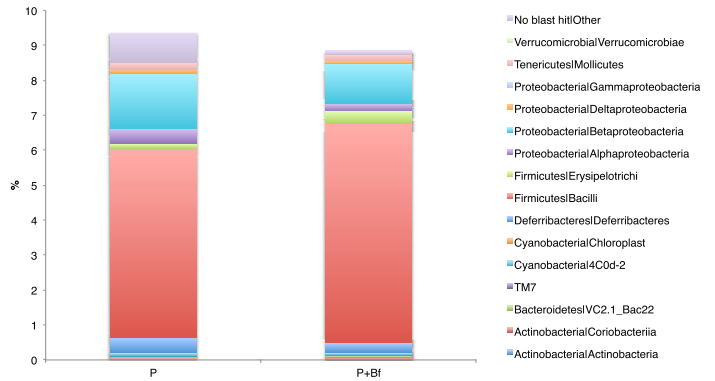
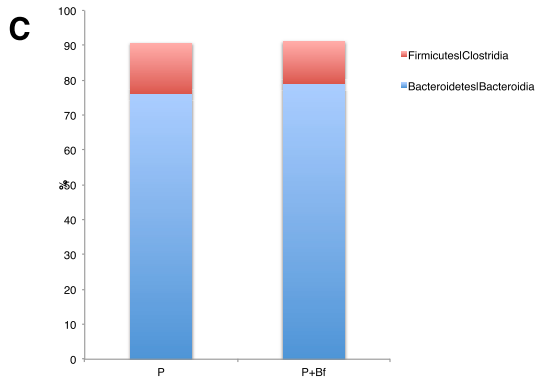
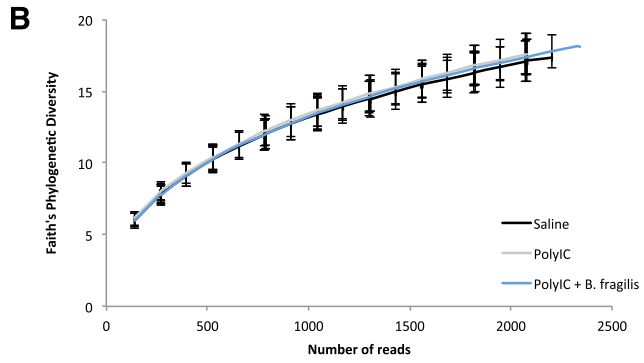
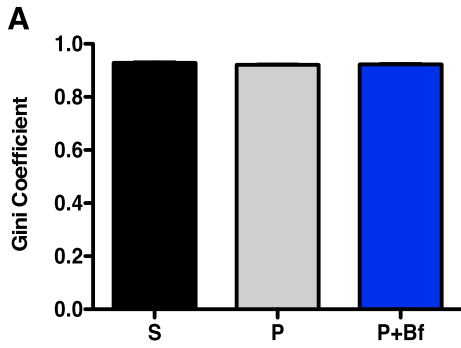
Figure S1. *B. fragilis* Treatment Has Little Effect on Tight Junction Expression and Cytokine Profiles in the Small Intestine, Related to Figures 1 and 3

(A) Expression of tight junction components relative to β -actin in small intestines of adult saline and poly(I:C) offspring. Data for each gene are normalized to expression levels in saline offspring. $n = 8/\text{group}$.

(B) Quantification of the effect of *B. fragilis* treatment on expression of notable tight junction components relative to β -actin in small intestines of MIA offspring. Data for saline and poly(I:C) are as in (A). $n = 8/\text{group}$.

(C) Protein levels of cytokines and chemokines relative to total protein content in small intestines of adult saline, poly(I:C) and poly(I:C)+*B. fragilis* offspring. Data are normalized to expression levels in saline offspring. Asterisks directly above bars indicate significance compared to saline control (normalized to 1, as denoted by the black line), whereas asterisks at the top of the graph denote statistical significance between poly(I:C) and poly(I:C)+*B. fragilis* groups. $n = 8-10/\text{group}$.

Data are presented as mean \pm SEM. * $p < 0.05$, ** $p < 0.01$, S = saline+vehicle, p = poly(I:C)+vehicle, P+BF = poly(I:C)+*B. fragilis*.



(legend on next page)

Figure S2. No Evidence for Persistent Colonization of *B. fragilis* after Treatment of MIA Offspring, Related to Figures 2 and 4

(A) Evenness of the gut microbiota, as indicated by the Gini coefficient. $n = 10/\text{group}$.

(B) Richness of the gut microbiota, as illustrated by rarefaction curves plotting Faith's Phylogenetic Diversity (PD) versus the number of sequences for each treatment group. $n = 10/\text{group}$.

(C) Mean relative abundance of OTUs classified by taxonomic assignments at the class level for the most abundant taxa (left) and least abundant taxa (right) for poly(I:C) versus poly(I:C)+*B. fragilis* treatment. $n = 10/\text{group}$.

(D) Levels of *B. fragilis* 16S sequence (top) and bacterial 16S sequence (bottom) in fecal samples collected at 1, 2, and 3 weeks posttreatment of adult offspring with vehicle or *B. fragilis*. Germ-free mice colonized with *B. fragilis* were used as a positive control. Data are presented as quantitative RT-PCR cycling thresholds [C(t)], where $C(t) > 34$ (hatched line) is considered negligible, and for $C(t) < 34$, lesser C(t) equates to stronger abundance. $n = 1$, where each represents pooled sample from 3-5 independent cages.

(E) Levels of *B. fragilis* 16S sequence (top) and bacterial 16S sequence (bottom) in cecal samples collected at 1, 2, and 3 weeks posttreatment of adult offspring with vehicle or *B. fragilis*. Germ-free mice colonized with *B. fragilis* were used as a positive control. Data are presented as quantitative RT-PCR cycling thresholds [C(t)], where $C(t) > 34$ (hatched line) is considered negligible, and for $C(t) < 34$, lesser C(t) equates to stronger abundance. $n = 1$, where each represents pooled sample from 3-5 independent cages.

Data are presented as mean \pm SEM. S = saline+vehicle, p = poly(I:C)+vehicle, P+BF = poly(I:C)+*B. fragilis*, GF+BF = germ-free+*B. fragilis*.

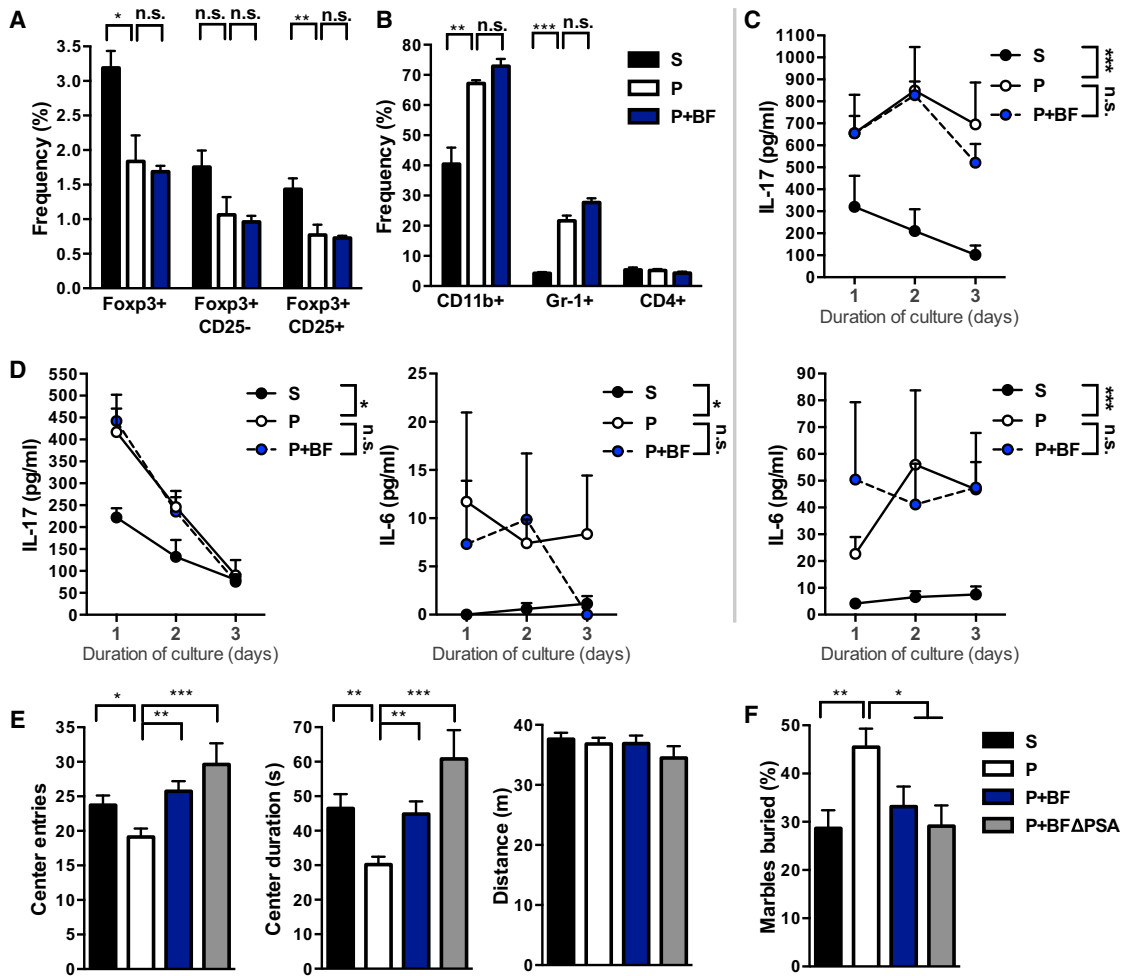


Figure S3. *B. fragilis* Treatment Has No Effect on Systemic Immune Dysfunction in MIA Offspring, Related to Figure 5

(A) Percent frequency of Foxp3+ CD25+ T regulatory cells from a parent population of CD4+ TCRb+ cells, measured by flow cytometry of splenocytes from adult saline, poly(I:C) and poly(I:C)+*B. fragilis* offspring. n = 5/group.

(B) Percent frequency of CD4+ T helper cells and CD11b+ and Gr-1+ neutrophilic and monocytic cells from a parent population of TER119- cells, measured by flow cytometry of splenocytes from adult saline, poly(I:C) and poly(I:C)+*B. fragilis* offspring. n = 5/group.

(C) Production of IL-17 and IL-6 by splenic CD4+ T cells isolated from adult saline and poly(I:C) offspring, after in vitro stimulation with PMA/ionomycin. Treatment effects were assessed by repeated-measures two-way ANOVA with Bonferroni post hoc test. n = 5/group.

(D) Production of IL-17 and IL-6 by CD4+ T cells isolated from mesenteric lymph nodes of adult saline and poly(I:C) offspring, after in vitro stimulation with PMA/ionomycin. Treatment effects were assessed by repeated-measures two-way ANOVA with Bonferroni post hoc test. n = 5/group.

(E) Anxiety-like and locomotor behavior in the open field exploration assay for adult MIA offspring treated with mutant *B. fragilis* lacking production of polysaccharide A (PSA). Data indicate total distance traveled in the 50 × 50 cm open field (right), duration spent in the 17 × 17 cm center square (middle) and number of entries into the center square (left) over a 10 min trial. Data for saline, poly(I:C) and poly(I:C)+*B. fragilis* groups are as in Figure 5. poly(I:C)+*B. fragilis* with PSA deletion: n = 17.

(F) Repetitive burying of marbles in a 6 × 8 array in a 10 min trial. Data for saline, poly(I:C) and poly(I:C)+*B. fragilis* groups are as in Figure 5. poly(I:C)+*B. fragilis* with PSA deletion: n = 17.

Data are presented as mean ± SEM. *p < 0.05, **p < 0.01, ***p < 0.001. S = saline+vehicle, p = poly(I:C)+vehicle, P+BF = poly(I:C)+*B. fragilis*, P+BFΔPSA = poly(I:C)+*B. fragilis* with PSA deletion.

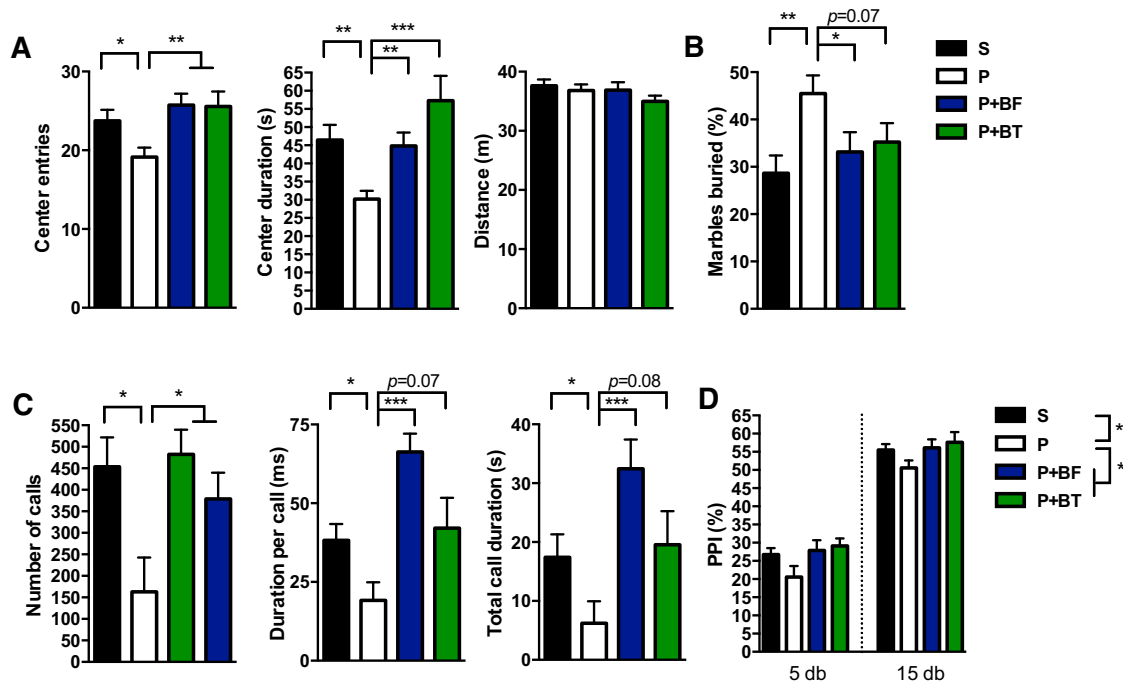


Figure S4. Amelioration of Autism-Related Behaviors in MIA Offspring Is Not Specific to *B. fragilis* Treatment, Related to Figure 5

(A) Anxiety-like and locomotor behavior in the open field exploration assay, as measured by total distance traveled in the 50 × 50 cm open field (right), duration spent in the 17 × 17 cm center square (middle), and number of entries into the center of the field (left) over a 10 min trial. Poly(I:C)+*B. thetaiotaomicronn*: n = 32.

(B) Repetitive burying of marbles in a 3 × 6 array during a 10 min trial. Poly(I:C)+*B. thetaiotaomicronn*: n = 32.

(C) Communicative behavior, as measured by total number (left), average duration (middle) and total duration (right) of ultrasonic vocalizations produced by adult male mice during a 10 min social encounter. Poly(I:C)+*B. thetaiotaomicronn*: n = 10.

(D) Sensorimotor gating in the PPI assay, as measured by percent difference between the startle response to pulse only and startle response to pulse preceded by a 5 db or 15 db prepulse. Treatment effects were assessed by repeated-measures two-way ANOVA with Bonferroni post hoc test. Poly(I:C)+*B. thetaiotaomicronn*: n = 32.

For all panels, data for saline, poly(I:C) and poly(I:C)+*B. fragilis* are as in Figure 5. Graphs represent cumulative results obtained for 3-6 independent cohorts of mice. Data are presented as mean ± SEM. *p < 0.05, **p < 0.01, ***p < 0.001. S = saline+vehicle, p = poly(I:C)+vehicle, P+BF = poly(I:C)+*B. fragilis*, P+BT = Poly(I:C)+*B. thetaiotaomicronn*.

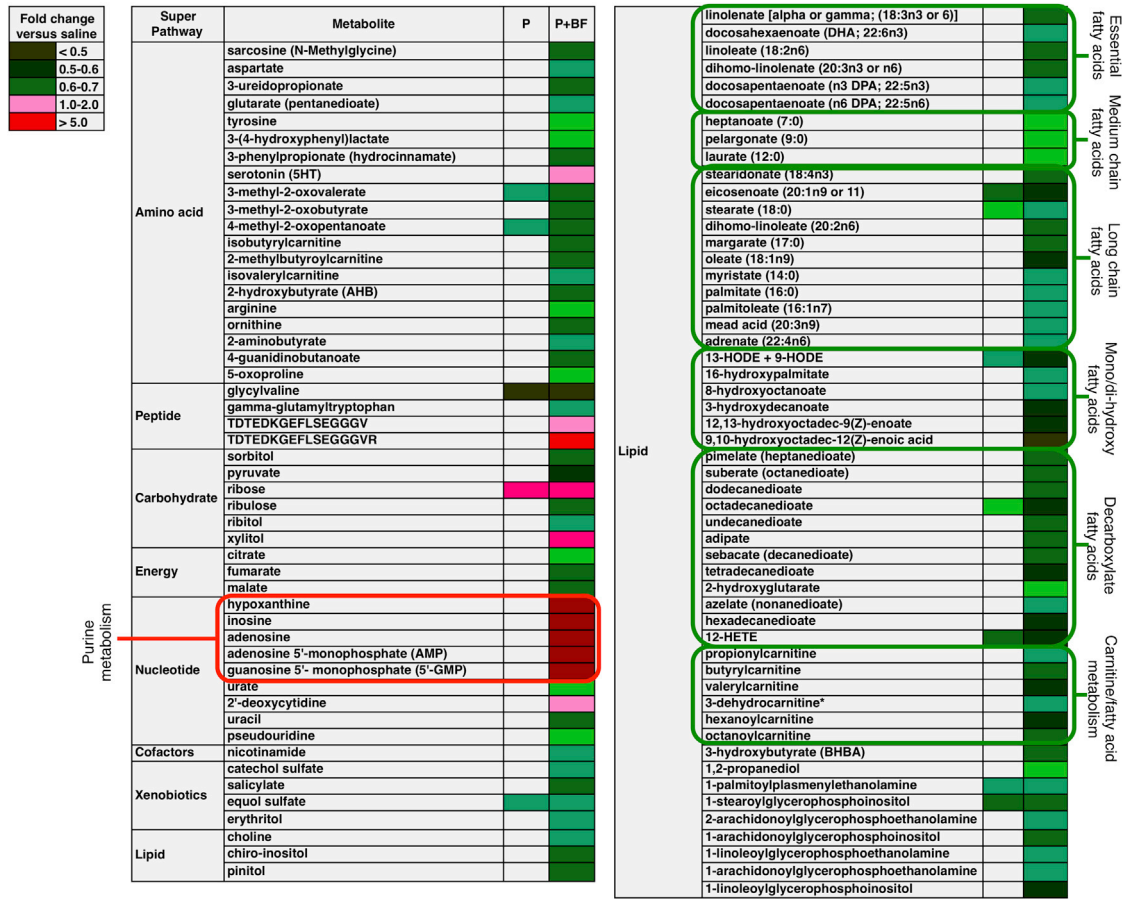


Figure S5. B. fragilis Treatment Causes Statistically Significant Alterations in Serum Metabolites, with Widespread Changes in Biochemicals Relevant to Fatty Acid Metabolism and Purine Salvage Pathways, Related to Figure 6

Levels of 103 metabolites that are significantly altered in sera of *B. fragilis*-treated MIA offspring compared to saline controls, as measured by GC/LC-MS. Colors indicate fold change relative to metabolite concentrations detected in saline offspring, where red hues represent increased levels compared to controls and green hues represent decreased levels compared to controls (see legend on top left). All changes indicated are $p < 0.05$ by two-way ANOVA with contrasts. $p = \text{poly}(I:C)$, $P+BF = \text{poly}(I:C)+B. fragilis$. $n = 8/\text{group}$.

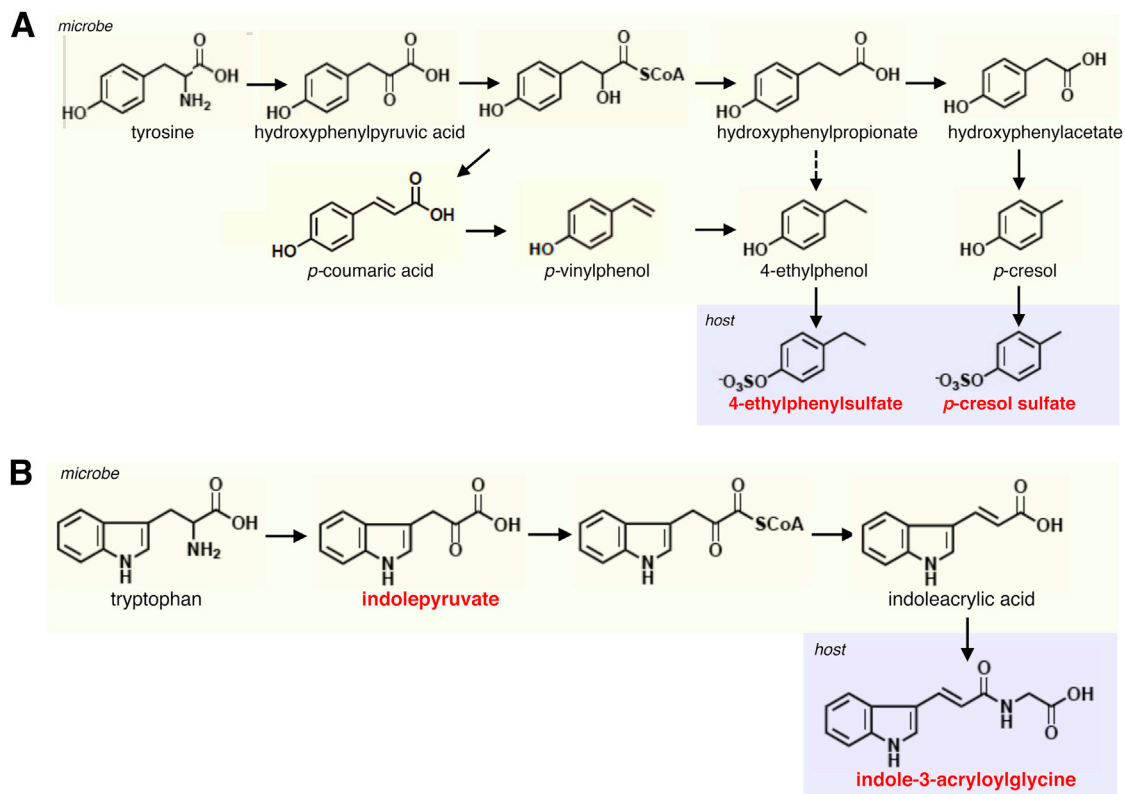


Figure S6. Synthesis of Autism-Associated Metabolites by Host-Microbe Interactions, Related to Figure 6

(A) Diagram illustrating the synthesis of 4EPS (found elevated in MIA serum and restored by *B. fragilis* treatment) and *p*-cresol (reported to be elevated in urine of individuals with ASD) by microbial tyrosine metabolism and host sulfation.

(B) Diagram illustrating the synthesis of indolepyruvate (found elevated in MIA serum and restored by *B. fragilis* treatment) and indole-3-acryloylglycine (reported to be elevated in urine of individuals with ASD) from microbial tryptophan metabolism and host glycine conjugation.

Solid arrows represent known biological conversions. Dotted arrow represents predicted biological conversions.

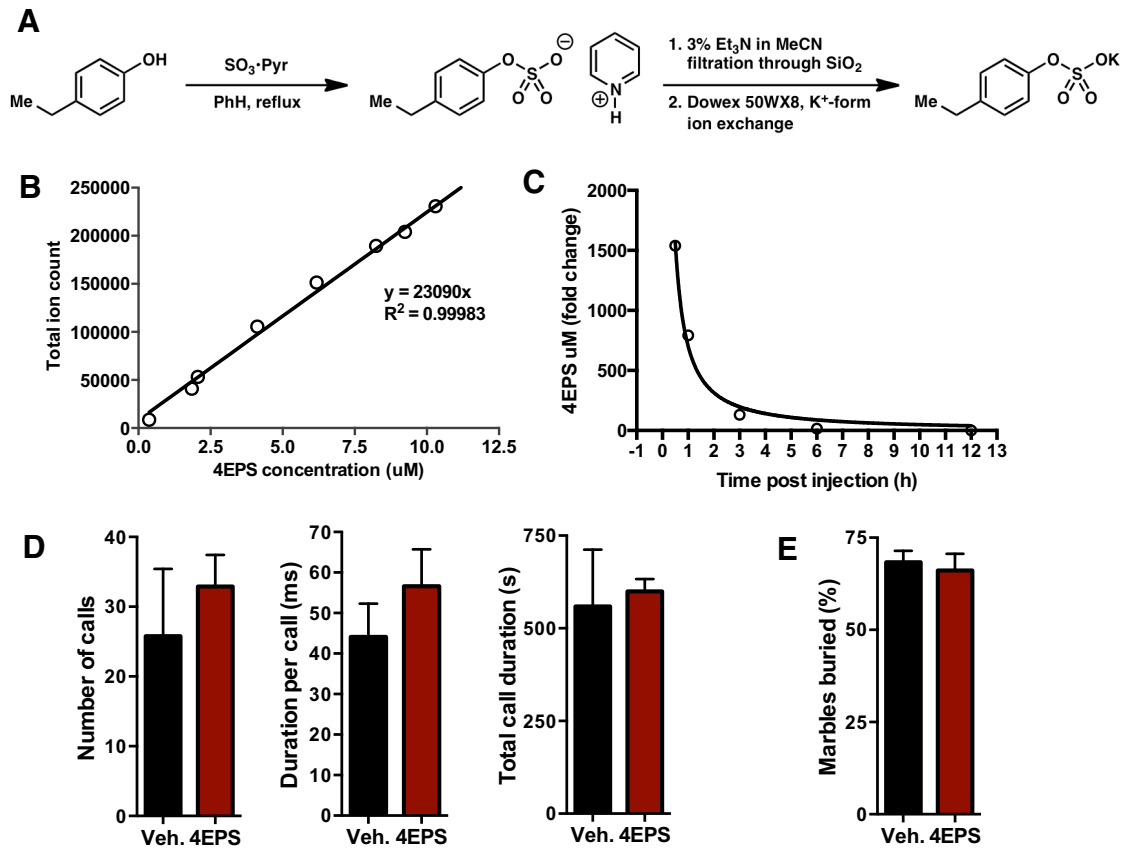


Figure S7. 4-ethylphenylsulfate Synthesis, Detection and In Vivo Experiments, Related to Figure 6

(A) Diagram of 4EPS synthesis by treating 4-ethylphenol with sulfur trioxide-pyridine in refluxing benzene to generate the pyridinium salt followed by ion exchange over K⁺ resin to generate the potassium salt.

(B) Dose-response curve and linear regression analysis for known concentrations of potassium 4EPS analyzed by LC/MS.

(C) Time-dependent increases in serum 4EPS after a single i.p. injection of 30 mg/kg potassium 4EPS into adult wild-type mice.

(D) Communicative behavior, as measured by total number (left), average duration (middle) and total duration (right) of ultrasonic vocalizations produced by adult male mice during a 10 min social encounter. *n* = 5/group.

(E) Repetitive burying of marbles in a 3 × 6 array during a 10 min trial. *n* = 10/group.

Data are presented as mean ± SEM. Veh. = vehicle (saline), 4EPS = 4-ethylphenylsulfate.